

## Article

# CO<sub>2</sub> Sequestration through Mineral Carbonation: Effect of Different Parameters on Carbonation of Fe-Rich Mine Waste Materials

Verma Loretta M. Molahid <sup>1,\*</sup>, Faradiella Mohd Kusin <sup>1,2</sup>, Sharifah Nur Munirah Syed Hasan <sup>1</sup>, Noor Allesya Alis Ramli <sup>1</sup> and Ahmad Makmom Abdullah <sup>1</sup>

<sup>1</sup> Department of Environment, Faculty of Forestry and Environment, Universiti Putra Malaysia, Serdang 43400, Selangor, Malaysia; faradiella@upm.edu.my (F.M.K.); muniraleeshara@gmail.com (S.N.M.S.H.); allesya301197@gmail.com (N.A.A.R.); amakmom@upm.edu.my (A.M.A.)

<sup>2</sup> Institute of Tropical Forestry and Forest Product (INTROP), Serdang 43400, Selangor, Malaysia

\* Correspondence: vermaloretta94@gmail.com; Tel.: +60-11-26770708



**Citation:** Molahid, V.L.M.; Mohd Kusin, F.; Syed Hasan, S.N.M.; Ramli, N.A.A.; Abdullah, A.M. CO<sub>2</sub> Sequestration through Mineral Carbonation: Effect of Different Parameters on Carbonation of Fe-Rich Mine Waste Materials. *Processes* **2022**, *10*, 432. <https://doi.org/10.3390/pr10020432>

Academic Editor: Federica Raganati

Received: 14 January 2022

Accepted: 12 February 2022

Published: 21 February 2022

**Publisher's Note:** MDPI stays neutral with regard to jurisdictional claims in published maps and institutional affiliations.



**Copyright:** © 2022 by the authors. Licensee MDPI, Basel, Switzerland. This article is an open access article distributed under the terms and conditions of the Creative Commons Attribution (CC BY) license (<https://creativecommons.org/licenses/by/4.0/>).

**Abstract:** Mineral carbonation is an increasingly popular method for carbon capture and storage that resembles the natural weathering process of alkaline-earth oxides for carbon dioxide removal into stable carbonates. This study aims to evaluate the potential of reusing Fe-rich mine waste for carbon sequestration by assessing the influence of pH condition, particle size fraction and reaction temperature on the carbonation reaction. A carbonation experiment was performed in a stainless steel reactor at ambient pressure and at a low temperature. The results indicated that the alkaline pH of waste samples was suitable for undergoing the carbonation process. Mineralogical analysis confirmed the presence of essential minerals for carbonation, i.e., magnetite, wollastonite, anorthite and diopside. The chemical composition exhibited the presence of iron and calcium oxides (39.58–62.95%) in wastes, indicating high possibilities for carbon sequestration. Analysis of the carbon uptake capacity revealed that at alkaline pH (8–12), 81.7–87.6 g CO<sub>2</sub>/kg of waste were sequestered. Furthermore, a particle size of <38 µm resulted in 83.8 g CO<sub>2</sub>/kg being sequestered from Fe-rich waste, suggesting that smaller particle sizes highly favor the carbonation process. Moreover, 56.1 g CO<sub>2</sub>/kg of uptake capacity was achieved under a low reaction temperature of 80 °C. These findings have demonstrated that Fe-rich mine waste has a high potential to be utilized as feedstock for mineral carbonation. Therefore, Fe-rich mine waste can be regarded as a valuable resource for carbon sinking while producing a value-added carbonate product. This is in line with the sustainable development goals regarding combating global climate change through a sustainable low-carbon industry and economy that can accelerate the reduction of carbon dioxide emissions.

**Keywords:** mineral carbonation; carbon sequestration; mine waste; Fe-rich waste; CCU; CCS

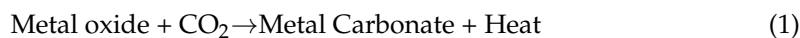
## 1. Introduction

Efforts to find a solution for the alarming climate change issue have resulted in research all over the world proposing large-scale carbon dioxide sequestration from the atmosphere [1]. As reported by National Oceanic and Atmospheric Administration (NOAA) [2], the carbon dioxide concentration has increased from 280 ppm in the 1970s to 402 ppm in 2016, mainly due to the increasing population and increasing activity of fossil fuel combustion. Recently, the monthly average of carbon dioxide concentration reached 416.71 ppm in December 2021 compared to the monthly average of 414.26 ppm in December 2020 [3]. It has been said that the atmospheric strain of carbon dioxide is now similar to 4.1–4.5 million years ago (in the course of the Pliocene Climatic Optimum), where carbon dioxide level was measured at approximately 400 ppm. Within that time, the average temperature was about 4 °C warmer than in pre-industrial times, and the global mean sea level was 23.5 m

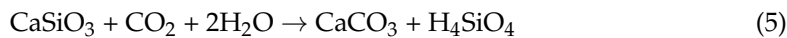
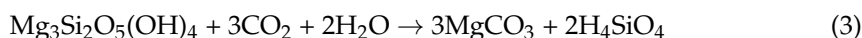
above the current level [4]. A study also reveals that a large forest area in the Arctic has transformed into a tundra-dominated region [5]. The fact that the level of carbon dioxide has become on par with one of the historical times of earth is alarming, as these changes can affect everything. This includes extreme weather that can affect the surrounding environment, humans and other living things. Concern over the global warming issue, specifically regarding the anthropogenic contribution (use of fossil fuel and carbon dioxide emission), gives rise to serious international demand on nations to lower their production of anthropogenic carbon dioxide. Leung et al. [6] have mentioned the different strategies many countries have used to decrease their carbon dioxide emissions, including carbon capture and storage.

Carbon sequestration, also known as carbon capture and storage (CCS), is used to explain both natural and man-made processes which involve getting rid of carbon dioxide from the atmosphere or diverting it from emission sources and storing it in geological formations, terrestrial environments (vegetation, soils, and sediments), and the ocean [7]. In general, the separated and captured carbon dioxide will be stored away in a storage site large enough relative to its annual emission so that it can significantly affect the carbon dioxide atmospheric concentration, such that carbon dioxide is isolated from the atmosphere for a very long time [8]. Possible storage methods include injection into the water column in the deep ocean, injection into underground geological formations (e.g., oil and gas fields, deep saline formations and unminable coal beds) or industrial fixation in inorganic carbonates, also known as mineral carbonation. Small amounts of captured carbon dioxide (6–8 g/L) were also used and stored in typical carbonated drinks in soft drink industries [9]. Years after CCS was introduced, an extension of it has been brought to light where, instead of only capturing and storing carbon, it can be utilized in the development of green products. This is also known as carbon capture and utilization (CCU). The product, which is manufactured with the captured carbon in it, can then be commercialized, for example, in the construction sector as supplementary cementitious materials for brick and concrete, and in other sectors as synthetic fuels; there are many more possible applications depending on the type of materials used [10–13]. Although the aim of CCS and CCU is to capture carbon emissions and to prevent them from being released back to the atmosphere, the last destination of the carbon dioxide captured marks the difference between both terms. CCS transfers the captured carbon dioxide to a chosen storage area for a long period of time, while CCU converts the captured carbon dioxide into a value-added product that can bring revenue to various sectors, such as bendable concrete, methane, urea and fuels [7,8,14–22]. Out of these potential CCS and CCU technologies, mineral carbonation has been suggested as an ideal approach where the carbon dioxide in the atmosphere can be stored and kept permanently as a stable and non-toxic carbonate product that can further be used and commercialized (e.g., partial cement replacement, brick production, paint and many more possibilities) [23–25]. This shows that mineral carbonation can act as a useful approach for both CCS and CCU, but the latter seems more promising, as it offers additional revenue in addition to removing carbon dioxide from the air.

Mineral carbonation is the reaction of basic minerals with carbon dioxide to form non-toxic solid carbonate. The carbonation process can occur naturally, but some modifications to accelerate this natural process can contribute to reducing the level of excess carbon dioxide in the atmosphere, thus reducing the global temperature. Mineral carbonation can be explained by the reaction of carbon dioxide with metal oxide-bearing minerals forming insoluble carbon, as shown in Equation (1) [26].



Generally, mineral carbonation reactions can occur with different starting materials, including Mg silicate, Fe silicate or Ca silicate. Equations (2)–(5) show the mineral carbonation process with Mg-, Fe- and Ca-rich silicates, respectively [26].



Mineral carbonation can be achieved either *in situ* or *ex situ*. The *in situ* method is when the carbon dioxide is stored underground when a reaction takes place between carbon dioxide and the reactive material, trapping the carbon dioxide as carbonate materials, whereas the *ex situ* reaction is the same as *in situ* but occurs above ground in a chemical processing plant [27]. Mineral carbonation is regarded as a promising solution for carbon sequestration, where the carbonates formed at the end of the reaction are non-hazardous to the environment and to humans and are in a stable form [23]. A study has shown that synthetic magnesium and calcium carbonate, when leached in nitric acid (which acts as acid rain), resulted in no significant release of carbon dioxide even in pH values less than 2 [28]. This shows that magnesium and calcium carbonate are stable and resistant enough to prevent carbon dioxide leakage when exposed to unexpected weather at their respective storage sites. This highlights the major advantages of using mineral carbonation to sequester carbon dioxide, i.e., it provides permanent carbon storage and is environmentally harmless. Furthermore, the material needed for mineral carbonation is abundant, and it exists worldwide as natural minerals, steel slag and red gypsum from industrial waste, and silicate minerals from mining waste. Yan et al. [29] studied the direct aqueous mineral carbonation of wollastonite ( $\text{CaSiO}_3$ ) and achieved a carbonation efficiency of 83.5% ( $150^\circ\text{C}$ , 40 bar and  $<30\text{ }\mu\text{m}$ ). Azdarpour et al. [30] used red gypsum in their study and achieved 12.53% efficiency ( $200^\circ\text{C}$ , 20 bar and  $<45\text{ }\mu\text{m}$ ) in 1 h, while Ukwattage et al. [31] achieved a carbonation efficiency of 8.83% using steel slag ( $50^\circ\text{C}$ , 0.19 MPa) in 48 h. Different types of materials were used in their study, resulting in different carbonation efficiencies. Yan et al. [29] have achieved the highest efficiency; the material they used was a targeted natural mineral containing high amounts of calcium oxide that allowed for more carbonation reactions to occur. It is worth noting that despite the various types of feedstock that can be used, the optimum condition for the carbonation reaction cannot be assumed to occur efficiently at certain fixed parameters, as it is found to be greatly dependent on the experimental conditions and material properties [31]. Therefore, it is crucial for a laboratory-scale experiment to be conducted so that it can be up-scaled into a pilot test and can be tested further in the industry.

Successful industrial applications, such as CarbonCure technology, a Canadian clean-tech company, have taken the interest of many parties, including local communities, as it can also generate income. Using this technology, more than 5 million cubic yards of concrete made with recycled carbon dioxide have been delivered to construction projects across the globe. Pan-United Corporation Ltd. Singapore [32] is the first company in Asia that has adopted CarbonCure technology; they hope to initiate an industry-wide movement to adopt more environmentally friendly practices in Singapore and the region [33]. CarbonCure Technologies (CarbonCure Technologies Inc., Halifax, NS, Canada), along with Mineral Carbonation International (Canberra, Australia) [34], Carbon8 Systems (Gillingham, UK) [35], and Solidia Technologies (Piscataway, NJ, USA) [36], are some of the companies which focus mainly on construction material production through the mineral carbonation process.

This study focuses on the utilization of mine waste materials as feedstock to capture carbon dioxide. The use of waste materials such as mining waste, steel slag, and fly ash in capturing carbon dioxide can be a beneficial approach, as this can help in solving the

problem associated with increasing carbon dioxide emissions from a carbon-intensive industry (the steel-making industry, limestone quarries, mining facilities) as well as the increasing waste land caused by the accumulated waste. It has been known that mining waste also contains low-grade ore, which may have economic value in the future [37]. In particular, utilizing mine waste to capture carbon can lower the impact of wastelands, hence reducing the environmental footprint (e.g., contamination of surface water caused by weathering of mining waste). The mining industry can also benefit from the utilization of its waste, as it may require less expenditure to close a mine for rehabilitation, closure and long-term monitoring [38].

The use of mining waste for mineral carbonation has been investigated in some related studies. For instance, Mohd-Isha et al. [39] studied the mineral carbonation potential of sedimentary limestone mine waste by evaluating the chemical and mineralogical properties of the waste. Molahid et al. [40] carried out the carbonation of limestone waste under ambient temperature and pressure. Both studies have shown that sedimentary limestone waste, which is naturally alkaline, has the potential to capture carbon dioxide, and usage of the waste can reduce the potential risk of mine waste to the environment and to human health. In addition, Hasan et al. [41,42] has investigated the potential of sediment, sludge and soil from gold mine waste, which consists of alkaline earth silicates. This study found that the availability of natural silicate minerals and the large fraction of small-sized particles makes it a suitable feedstock for passive mineral carbonation. However, a carbonation experiment needs to be carried out in order to confirm the claim based on the characterization analysis. On the other hand, Ramli et al. [43] performed a carbonation experiment of iron ore mining waste at a pressure of 1 bar, and have proved that carbonation can be conducted in low-pressure conditions. They have also stated that temperature, pH and particle size are important in the carbonation process. However, other variables could be included or accelerated to enhance carbonation efficiency.

Although numerous studies have been done on mineral carbonation, only a few have used mine waste material in low pressure (1–10 bar) and temperature conditions (80 °C–200 °C), and research on this aspect of carbon sink is still limited [39–43]. Therefore, this study aims to evaluate the potential of using Fe-rich mine waste for carbon sequestration and to assess the different factors influencing the carbonation process, i.e., pH conditions, particle size fractions and reaction temperature. This would be useful for giving insights into the application of CCS/CCU technology that incorporates waste materials for environmental sustainability.

## 2. Materials and Methods

### 2.1. Materials Preparation

In this study, Fe-rich mine waste collected from an iron ore mine site in Jerantut, Pahang were used. The mine wastes were discarded and disposed of in stockpiles and tailings, which were regarded as waste materials. The waste samples were collected from five sampling locations, i.e., pond 1, pond 2, pond 3, tailings and waste dump. All of the samples were ascertained according to Smith et al. [44], in which samples were collected from the surface to a depth of approximately 15–20 cm to ensure that representative samples were obtained. All samples were gathered in a polythene bag separately using a stainless steel scoop ideal for sampling soil, sludge and sediment.

Sediments from tailings were air-dried at room temperature and were left approximately 24 h; rock samples were crushed using a geological hammer and were then ground. The air-dried soil, sludge and sediment were ground using an agate mortar and pestle. The waste materials were then sieved according to the chosen particle size fraction prior to the sample characterization analysis (<2 mm) and carbonation experiment (<38 µm, <63 µm, <75 µm).

### 2.2. Materials Characterization Analysis

The pH of the waste materials was measured according to British Standard (BS) 1377, Part 3 [45]. A solid to liquid ratio of 1:2.5 was used; samples and distilled water were mixed

and were left for 24 h, and the pH was then measured using a calibrated Orion 230A Plus Portable pH meter. To identify the crystalline phase, the waste materials were analyzed by X-ray diffraction (XRD) using a Bruker-AXS D8 Advanced diffractometer. Scans were taken at a rate of  $1^\circ/\text{min}$  ( $0.025^\circ$  step size), counting for 0.2 s per step over the  $5\text{--}50^\circ$  scattering angle range. The integrated intensity of peak areas was determined using Diffrac AT EVA software (v.9.0). The d-spacing was identified using OriginPro 9.55 software (Originlab Corporation, Northampton, UK).

A scanning electron microscope (SEM) (model Phillips XL30, Amsterdam, The Netherlands) equipped with an energy-dispersive X-ray (EDX) analyzer was used to determine the morphological structure of materials at 100–1000 magnification and the chemical composition in percentage (%). It is important to identify the chemical composition of the waste materials, as this can confirm the presence of the key oxide compounds (i.e., Ca/Mg/Fe oxide) needed in the carbonation process, while the SEM analysis helps in confirming the presence of these compounds through a magnified image of the waste materials by identifying the shapes or microstructure of the images.

### 2.3. Mineral Carbonation Experiment

The carbonation experiment was carried out in a designated reactor system (Donewell Equipment, model ACL03-250) with 250 mL working volume (Figure 1). The reactor consists of a heating mantle, gas inlet, outlet and pressure relief valve, removable Teflon cup, pressure indicator, and overhead stirrer with an analog control knob. The temperature was controlled using a digital temperature PID control with a maximum temperature of  $200\text{ }^\circ\text{C}$ , while the pressure was controlled using a pressure regulator with an output gauge range of 1–16 bar.

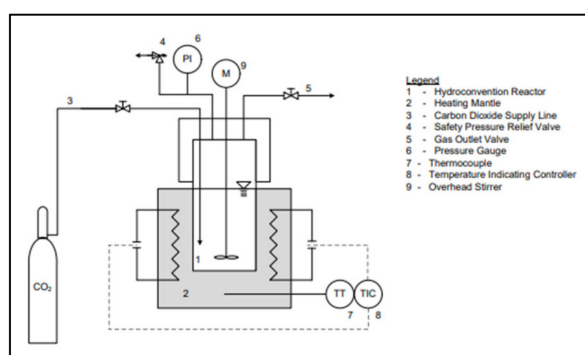


**Figure 1.** Schematic diagram of the reactor system.

The weighed amount of the waste materials was placed into the removable Teflon cup, to which was then added 1 M of sodium chloride (NaCl) and 0.64 M of sodium bicarbonate (NaHCO<sub>3</sub>) solution; these act as a catalyst to the reaction rates [46]. pH was then adjusted accordingly using sodium hydroxide (NaOH) or hydrochloric acid (HCl). The Teflon cup was placed inside the reactor and sealed tightly. When the reactor reached the desired temperature, it was filled with carbon dioxide gas with 99.8% purity (purchased from Smart Biogas Ent., Selangor). The reactor was run at a pressure of 1 bar, controlled by the gas feeding system, and the stirrer was set at 300 rpm. Each parameter tested was carried out for 60 min while the pressure, temperature, stirring rate and solution used were kept constant. The effects of pH conditions (i.e., 8, 10 and 12), particle size fractions (i.e., <38  $\mu\text{m}$ , <63  $\mu\text{m}$  and <75  $\mu\text{m}$ ) and reaction temperature (i.e.,  $80\text{ }^\circ\text{C}$ ,  $150\text{ }^\circ\text{C}$  and  $200\text{ }^\circ\text{C}$ ) were evaluated at ambient CO<sub>2</sub> pressure (1 bar). All experiments were replicated to ensure the quality of the results obtained.

### 2.4. Carbonation Product Analysis

Thermogravimetric analysis (TGA) (Mettler Toledo TGA/DSC 1), with a temperature range of  $30\text{ }^\circ\text{C}$ – $1000\text{ }^\circ\text{C}$  was carried out, and the carbon uptake capacity (%) and

sequestration capacity (g/kg) were calculated based on the weight loss obtained. The carbon uptake capacity (%) was calculated in reference to Azdarpour et al. [30] as shown in Equations (6) and (7), while carbon uptake capacity was calculated based on the stoichiometric equation assuming the decarbonation reactions in Equations (8)–(10), at the respective temperatures. Depending on the reaction condition, the temperature at which the carbonate product decomposes may vary or shift because of its thermal stability. Hence, the weight loss for  $\text{FeCO}_3$  and  $\text{CaCO}_3$  is not only subjected to a certain temperature [47–56]. For Equations (6) and (7),  $x$  is either Fe, Ca or Mg, and MW refers to molecular weight.

$$x \text{ uptake capacity (\%)} = \frac{x \text{ mass in } x\text{CO}_3}{x \text{ Total in feeding material}} \times 100 \quad (6)$$

$$x \text{ mass in } x\text{CO}_3 = \text{weight loss (\%)} \times \frac{\text{MW}_x}{\text{MWCO}_2} \times \text{mass of solid residue} \quad (7)$$

To further confirm the presence of carbonate, the thermogravimetric analysis and the differential thermogravimetry (TGA/DTG) curve were analyzed, and SEM-EDX was performed to confirm the presence of the carbonate mineral by analyzing the shape or structure of the carbonates.



### 3. Results and Discussion

#### 3.1. Waste Material Properties

The initial pH of the waste material was measured for the initial evaluation, as pH plays an important role in the mineral carbonation process [30,57,58]. For Fe-rich mine waste, most of the waste materials from different sampling sites have a pH between 7.0 to 7.5. This indicates that the material is alkaline in nature. It has been stated that materials that are alkaline in nature are essential to facilitate mineral precipitation for carbonation [13,43]. A study by Park and Fan [59] proved that precipitation was enhanced in a highly alkaline condition (i.e., pH 9.4), producing a magnesium carbonate product with high purity. This was also supported by other studies which added sodium hydroxide (NaOH) into their solution to increase the pH and the precipitation rate [40,41,46]. Based on the results obtained, all samples have an alkaline pH, suggesting that the natural pH of the mine waste shows great potential to be used as feedstock for the mineral carbonation process. Based on these past studies, pH condition can be seen as a crucial factor in the mineral carbonation process because altering the pH can further identify at which pH level mineral carbonation can be accelerated.

XRD analysis was carried out to identify potential minerals in the waste materials to undergo the carbonation reaction (i.e., Fe-, Mg-, and Ca-based minerals). XRD results of a few samples of Fe-rich waste are presented in Figure 2. The XRD pattern exhibits a significant pattern for amorphous (non-crystalline) material with several peaks of crystalline phases [60]. Quartz is the most abundant mineral, followed by anorthite ( $\text{CaAl}_2\text{Si}_2\text{O}_8$ ). The Fe-, Mg-, and Ca-based minerals which are crucial for the carbonation reaction are anorthite ( $\text{CaAl}_2\text{Si}_2\text{O}_8$ ), wollastonite ( $\text{CaSiO}_3$ ), diopside ( $(\text{Ca}(\text{Mg}, \text{Al})(\text{Si}, \text{Al})_2$ ), perovskite ( $\text{CaTiO}_3$ ), johannsenite ( $\text{Ca}_4\text{Mn}_4\text{Si}_8\text{O}_{24}$ ), magnesium aluminium silicate ( $\text{MgO}\cdot\text{Al}_2\text{O}_3\cdot\text{SiO}_2$ ), magnetite ( $\text{Fe}_3\text{O}_4$ ) and hematite ( $\text{Fe}_2\text{O}_3$ ). Among these, the most commonly used minerals for mineral carbonation are magnetite and wollastonite [30,40,43,47,61].

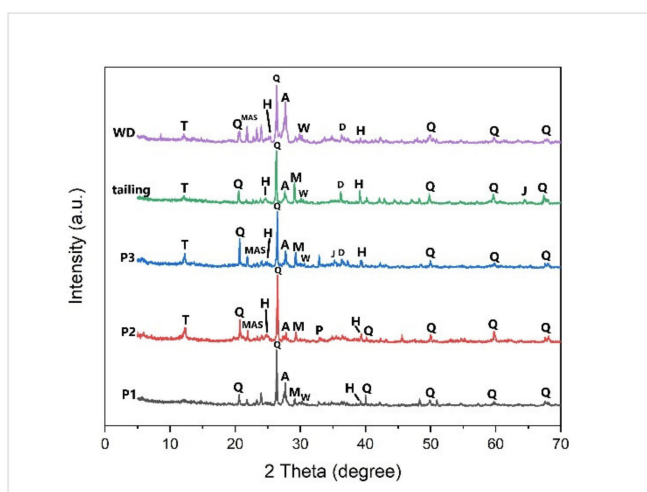
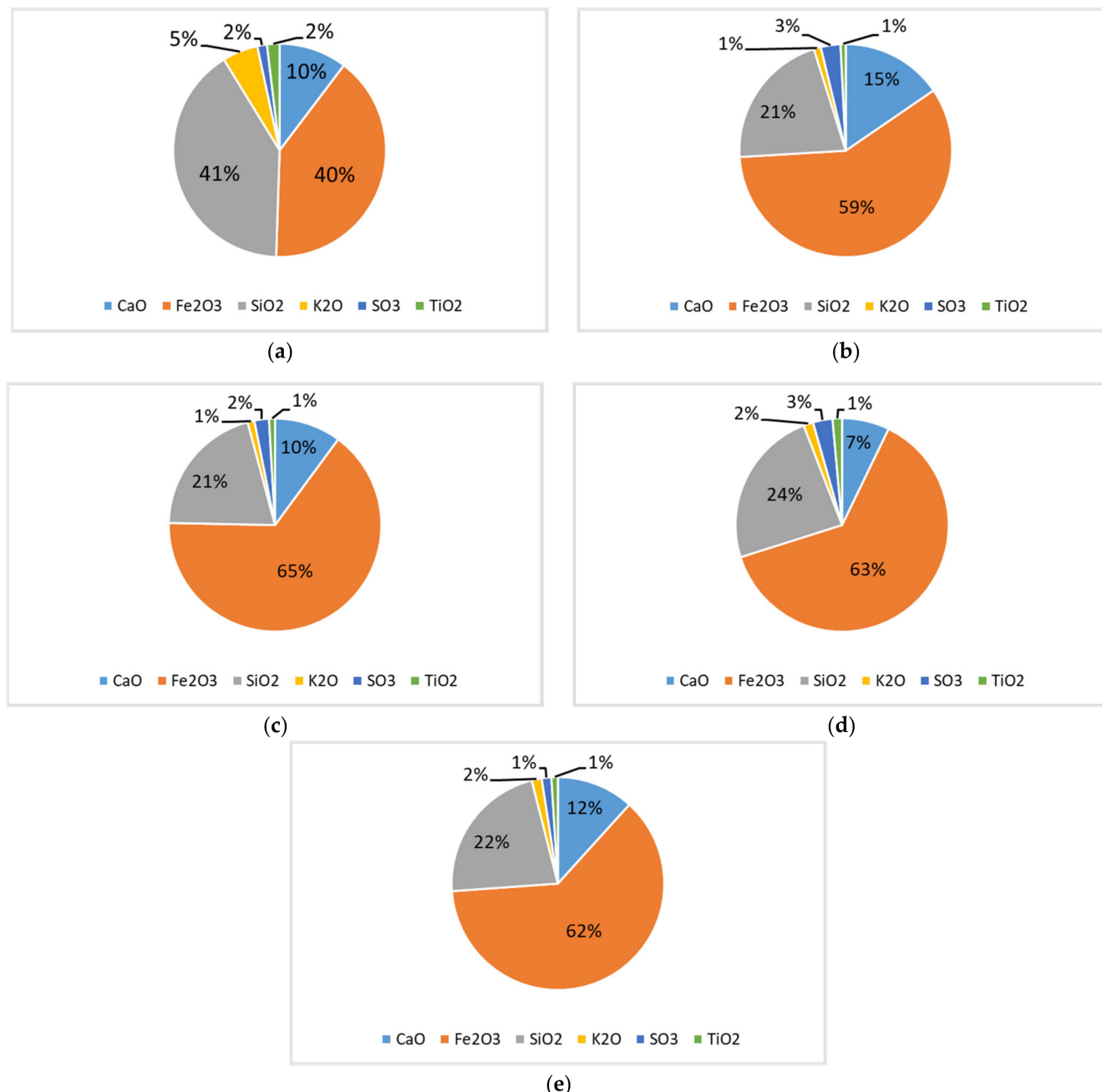


**Figure 2.** Raw Fe-rich mine waste X-ray diffractograms patterns of waste dump (WD), tailing, pond 1 (P1), pond 2 (P2), and pond 3 (P3). Labelled alphabet represents the minerals found in the waste: quartz (Q), anorthite (A), wollastonite (W), diopside (D), titanium silicon (T), magnetite (M), perovskite (P), magnesium aluminium silicate (MAS), johannsenite (J) and hematite (H).

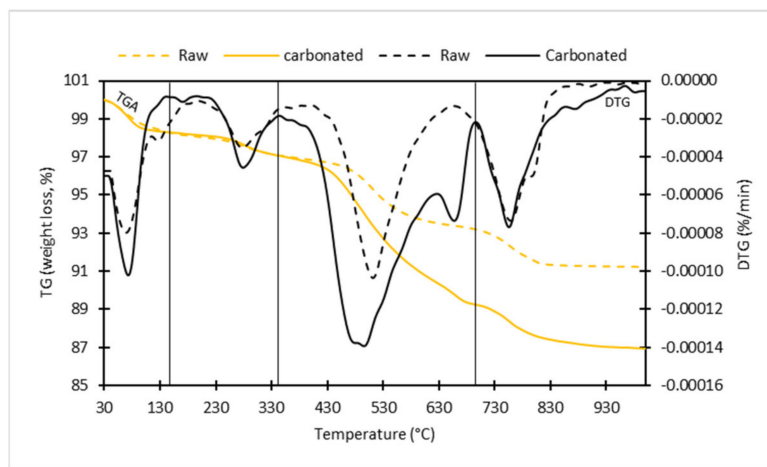
Obviously, the major oxide constituent in all samples was  $\text{Fe}_2\text{O}_3$  (also known as hematite). Figure 3 summarizes the chemical composition of the iron mine waste in five sampling locations; the iron mine waste was composed of  $\text{CaO}$ ,  $\text{Fe}_2\text{O}_3$ ,  $\text{SiO}_2$ ,  $\text{K}_2\text{O}$ ,  $\text{SO}_3$ , and  $\text{Al}_2\text{O}_3$ . The major oxide constituent was  $\text{Fe}_2\text{O}_3$  in all sampling locations; pond 1 has the highest percentage of 62.95%, followed by pond 2 (61.68%), pond 3 (61.05%), tailings (57.79%), and waste dump, with the lowest percentage of 39.58%. Therefore, the abundance of  $\text{Fe}_2\text{O}_3$  is indicative of the iron ore mineral composition. This is consistent with XRD analysis, where a hematite ( $\text{Fe}_2\text{O}_3$ ) peak was also discovered, although the detected minerals were found as a minor peak in all of the sampling locations. The only explanation for the lack of peak intensity is that  $\text{Fe}_2\text{O}_3$  probably exists in a non-crystalline form, also known as an amorphous form [62]. This explains the significant amorphous material pattern found in XRD curves in all sampling sites. Generally, amorphous material consists of small particles and is not as well-structured as crystalline material. This was probably due to the force applied during crushing and grinding of the samples, altering the samples' original structure. Azdarpour et al. [30] and Azdarpour et al. [63] experienced the same effect, where  $\text{Fe}_2\text{O}_3$  was one of the major compounds detected through XRF, but its peak was absent in the XRD curves. However, TGA was able to confirm the presence of  $\text{Fe}_2\text{O}_3$  in the raw sample (Figure 4), where a peak in the temperature interval of 200 °C–400 °C was detected, which can be attributed to the thermal decomposition of  $\text{Fe}_2\text{O}_3$  [52].

Figure 5 shows the SEM image of the Fe-rich mine waste. Based on the figure, the samples seem to have an irregular and highly rough surface. The porous structure of the samples can be observed, in which, according to [64,65], the structure can be associated with the presence of hematite and magnetite. This is consistent with the mineralogical and chemical composition analysis, which has also detected magnetite and hematite minerals in the samples. The second highest oxide constituent is  $\text{SiO}_2$ , which is silica. It is found mainly as quartz in the mine waste, and it is a major mineral found through XRD analysis, which explains the abundance of the oxide. Silica was considered a common impurity, also known as a gangue material, the existence of which can affect the quality of the ore [66]. Thus, the high silica composition explains why the raw mine waste was considered waste material. On the other hand,  $\text{CaO}$  with a percentage range of 7.19–15.24% was found in all sampling points, where the highest  $\text{CaO}$  content was in the tailings, while the lowest was in pond 2. The presence of  $\text{CaO}$  can be associated with the Ca-based minerals found in the waste (i.e., anorthite, diopside, perovskite, wollastonite and johannsenite). Clearly, the two important oxides found in the raw iron mine waste were  $\text{CaO}$  and  $\text{Fe}_2\text{O}_3$ . Each oxide was

present in all samples, and this consistency shows that this material has the potential to act as the feedstock in the mineral carbonation reaction.



**Figure 3.** Chemical composition of (a) waste dump, (b) tailing, (c) pond 1, (d) pond 2, and (e) pond 3.



**Figure 4.** Thermogravimetric (TG) analysis and DTG curve of carbonated Fe–rich mine waste (raw and particle size  $<38\text{ }\mu\text{m}$ ).

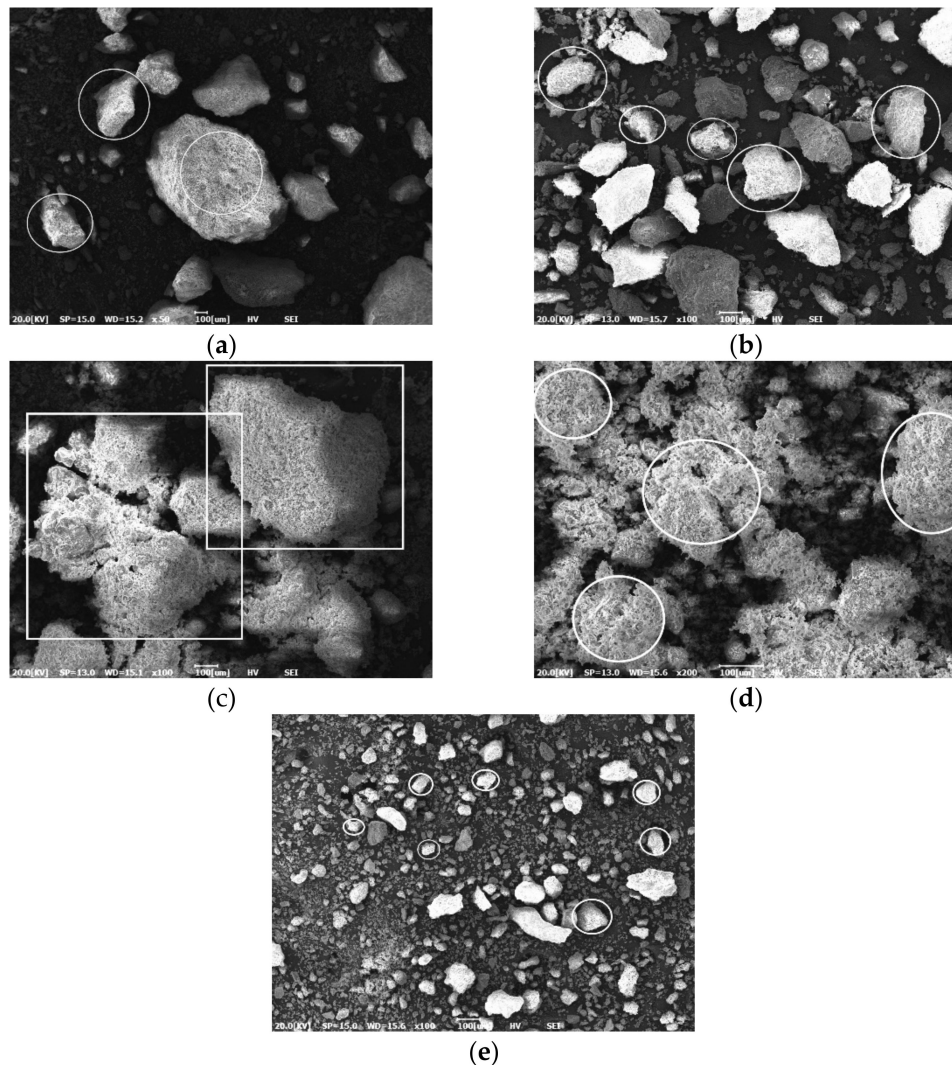


**Figure 5.** Micrograph of the Fe-rich mine waste samples from: (a) waste dump, (b) tailings, (c) pond 1, (d) pond 2, and (e) pond 3. The round and square shapes depict the porous magnetite minerals present in the raw Fe-rich mine waste.

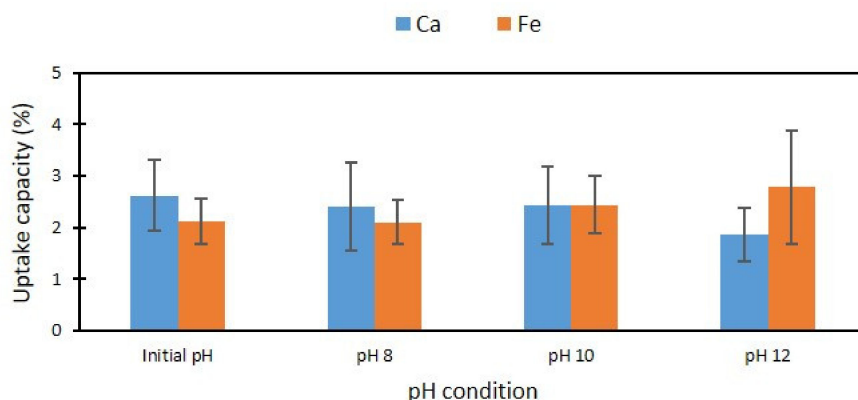
The high percentage of  $\text{Fe}_2\text{O}_3$  and some  $\text{CaO}$  (i.e., 39.58–62.95% and 7.19–15.24%, respectively), and also the presence of essential minerals for carbonation such as magnetite, anorthite, wollastonite, diopside, perovskite, johannsenite, and magnesium aluminium silicate ( $\text{MgO}\cdot\text{Al}_2\text{O}_3\cdot\text{SiO}_2$ ), in the waste signifies its potential to undergo a carbonation reaction, which involves the formation of iron carbonate and calcium carbonate as the final products, respectively. This also implies that the high amount of oxide minerals (i.e., calcium oxide and iron oxide) in the waste materials has the potential to store more carbon dioxide because of its high storage reserve for capturing and storing carbon dioxide.

### 3.2. Carbonation Process Optimization: Effect of Different Parameter Conditions on Carbon Uptake Capacity (%)

#### 3.2.1. Influence of pH on Uptake Capacity

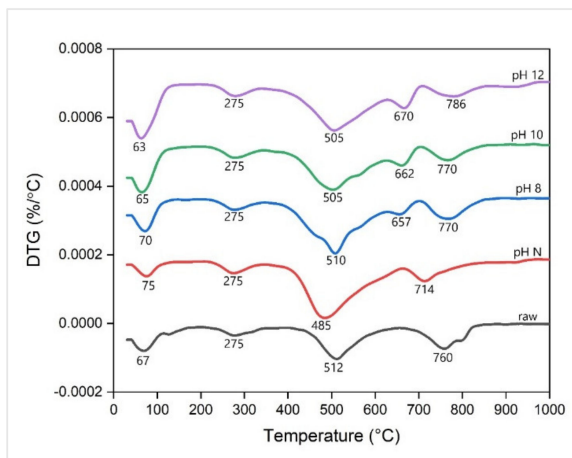
One of the controlling factors that can affect the carbon uptake capacity (%) is the availability of the divalent cation ( $\text{Ca}^{2+}$ ,  $\text{Mg}^{2+}$ ,  $\text{Fe}^{2+}$ ). The reason is that the dissolution of these metals would make it accessible for the carbon dioxide ( $\text{CO}_2$ ) gas to react with and form carbonate precipitates [26,67,68]. Thus, an optimum pH is needed for the metals to dissociate and become available for the carbonation process to take place. A previous study has proven that salinity and pH can significantly improve mineral carbonation when the pH condition is altered, specifically using pH values of 4, 6 and 10. Based on their results, where newly formed carbonate minerals were observed, it was concluded that altering the pH is a good method for improving the interaction of metal cations and carbon dioxide in an aqueous solution containing samples [68]. The effect of pH conditions on the carbonation process was investigated by altering the pH of the samples using  $\text{NaOH}$  and  $\text{HCl}$ . This was done so that the optimum pH for carbon uptake can be determined and the effect of pH on the carbonation process can be observed.

Figure 6 shows the average Ca and Fe uptake capacity. As shown in the figure, Ca carbon uptake seems to decrease with increasing pH, with uptake capacities of 2.62%, 2.41%, 2.39% and 1.86% for pH N, pH 8, pH 10 and pH 12, respectively. For Fe carbon uptake, the trend of increasing uptake capacity with increasing pH can be seen, with uptake capacities of 2.11%, 2.19%, 2.44% and 2.78% for pH N, pH 8, pH 10 and pH 12, respectively. It is well-known that low pH (acidic conditions) favors the liberation of the metal ions (i.e., Mg, Ca and Fe ions) from its minerals or current structure with the help of the  $\text{H}^+$  ion from the reaction of carbon dioxide gas and water. When this happens, metal ions will react with bicarbonate ions ( $\text{HCO}_3^-$ ) and finally precipitate as solid carbonate [25,46,49]. High pH condition favors the carbonate precipitation stage, where carbonate ion ( $\text{CO}_3^{2-}$ ) concentrations are higher [46,69]. Azdarpour et al. [63] and Wang et al. [70] have also stated that the precipitation stage to solid carbonate is greatly dependent on carbonate ( $\text{CO}_3^{2-}$ ) and bicarbonate ( $\text{HCO}_3^-$ ) ions in the solution. Hence, it is also favorable to increase  $\text{CO}_3^{2-}$  ion concentrations by increasing the pH. From this study, the Ca uptake capacity has a decreasing trend towards increasing pH condition, while the Fe uptake capacity has an opposite result: the uptake capacity increases with increasing pH. This can be explained by the chemical composition difference of iron oxide and calcium oxide, as calcium oxide has a low percentage amount compared to iron oxide. In the case of Ca carbonation, the problem arises when the pH is too high and no  $\text{H}^+$  ion is left to liberate Ca ions from the mineral because it has been neutralized by the excess  $\text{OH}^-$  ions. The low amount of calcium oxide in the waste material lowers the potential for it to be liberated. Although this condition is favorable for the precipitation of carbonate to occur because of the high  $\text{CO}_3^{2-}$  concentration, there are no available  $\text{Ca}^{2+}$  ions for it to react with. The dissolution of Ca, Mg, or Fe silicate minerals into the solution is, therefore, one of the rate-limiting factors [26]. For Fe uptake, compared to calcium oxide, iron oxide has more potential to be liberated into the solution because of its high constituent. Thus, the condition favors the carbonation process, which is in good agreement with previous studies that have agreed that the most suitable pH for mineral carbonation is greater than 10 [71].



**Figure 6.** Average uptake capacity (%) for different pH conditions of Fe-rich mine waste. Error bars represent standard error of the mean (SEM).

Figure 7 illustrates the DTG curves of raw and carbonated Fe-rich mine waste at initial pH (pH N) and at pH 8–12, which represent the peaks of weight loss that occurred in the temperature interval between 30–1000 °C. Most of the peaks appear at almost similar temperatures but have different weight loss percentages. The first peak can be identified in temperatures below 100 °C for raw and all carbonated Fe-rich waste samples, which can be identified as moisture loss and decomposition of some low-grade calcium silicate hydrate (C-S-H), as stated in the previous literature [50]. It can be seen that mass loss between 200 and 340 °C is common in all samples, with a peak at around 275 °C that corresponds to the thermal decomposition of iron hydroxide [51]. Following this peak, all samples started to exhibit different peaks starting from 340 °C. At the temperature interval of 340–660 °C, the raw and carbonated samples of pH N shows a strong peak with a high weight loss disparity of 3.72% and 8.04%, respectively. On the other hand, peaks observed for pH 8–12 were at temperatures of 340–630 °C and were closely followed by another peak at around 630–700 °C. According to El-Bellihi [53] and Stopic et al. [48], this can be attributed to the thermal decomposition of carbonate product, which can be seen in the temperature interval around 340–660 °C for pH N with a weight reduction of 8.04% and 340–630 °C for pH 8–12 with a weight reduction of 6.84%, 6.43% and 6.84%, respectively. A small peak around temperatures of 630–700 °C in pH 8–12 can be ascribed to the reduction of ferric oxide ( $\text{Fe}_2\text{O}_3$ ) or residuals from iron carbonate thermal decomposition into magnetite ( $\text{Fe}_3\text{O}_4$ ) [47,51]. Another noticeable peak was evident at around 660–1000 °C for pH N, and around 700–1000 °C for pH 8–12, which indicates calcium carbonate decarbonation, according to the literature [54].



**Figure 7.** DTG curves of raw and carbonated Fe-rich mine waste samples at initial pH, pH 8, pH 10 and pH 12.

In short, altering pH conditions to ensure optimum carbonation reactions requires a delicate balance between improving the extraction of cations from their respective minerals and enhancing the precipitation of the solid carbonate. In this case, these two opposite effects of pH can cause both to compete with each other, which in the end, produces different results from the one that has been expected. However, the addition of NaOH and NaHCO<sub>3</sub> can be considered adequate, such that no further altering of pH is needed. This is due to the lack of statistically significant differences found in uptake capacity using different pH values, showing that the chosen pH range (i.e., pH 7–12) has more or less the same effect on the carbonation process. This suggests that alkaline conditions are favorable for the reaction to occur.

### 3.2.2. Influence of Particle Size Fraction on Uptake Capacity

Figure 8 shows the average Ca and Fe uptake capacity (%) using different particle size fractions. Based on the figure, particle size reduction shows great potential in improving the uptake capacity (%). Particle size fractions <38 μm show a higher carbon uptake than particle size fractions <63 μm and <75 μm for both Ca and Fe. Figure 8 demonstrates that the uptake capacity follows a decreasing trend when the particle size increases in all the samples. Ca and Fe uptake capacities of 3.05% and 3.97%, respectively were achieved when using samples with a particle size of <38 μm. Uptake capacities of 2.04% and 3.31% for Ca and Fe, respectively, were obtained using a particle size of <63 μm. On the other hand, the lowest Ca and Fe uptake capacity was achieved using samples with a particle size <75 μm, with carbon uptake of 1.42% and 2.61%, respectively. Significant differences ( $p < 0.05$ ) in uptake capacity using different particle size fractions were found. Dunn–Bonferroni pairwise tests revealed a statistically significant difference in mean ranks between particle sizes of 38 μm and 75 μm. This means that using 38 μm or 75 μm particle size fractions will give different results of uptake capacity (%). Spearman’s rank-order correlation test also reveals a statistically significant, negative correlation between uptake capacity (%) and particle size used ( $r = -0.487, p = 0.006$ ), which proved that smaller particle size fractions increase the uptake capacity of the Fe-rich waste sample.

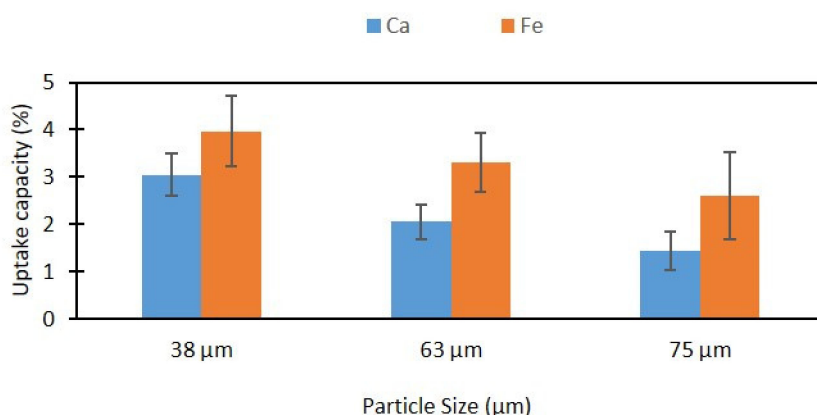


**Figure 8.** Average uptake capacity (%) for different particle size fractions of Fe-rich mine waste. Error bars represent standard error of the mean (SEM).

The TGA and DTG curves of a raw Fe-rich mine waste material compared with the <38 μm carbonated waste material are illustrated in Figure 4 in the characterization analysis of the previous section. Each peak of the DTG curve illustrates the stages of decomposition that occurred in the fresh and carbonated sample, where both samples have 4 different peaks separated by lines. The total weight loss for the raw sample of Fe-rich mine waste in the temperature interval of 30–1000 °C adds up to 8.78%, which connotes the amount of bound water and decomposed compound material due to the reaction with the heat applied. The total weight loss for the first and second peaks in the raw sample between 30–150 °C and 150–340 °C is 1.74% and 1.16%, compared with 3.63% and 1.36% for the carbonated

sample, respectively. The weight loss that occurred in the first peak was due to the water loss in both samples [48], and the carbonated sample seems to have higher moisture content than the raw sample. The second peak can be related to the dehydroxylation of the iron hydroxide, which was present in both samples [51]. The carbonated sample has slightly higher weight loss, which means that the carbonated sample has a higher amount of iron hydroxide due to the addition of sodium hydroxide in the carbonation experiment, forming more iron hydroxide.

Contrarily, in raw waste material, a weight reduction of 9.02% in the temperature region of 340–700 °C with a peak at 498 °C was observed. This can be observed in the figure where the largest peak (third peak) was noticeable, which indicates that this temperature interval is important because this is where the thermal decomposition of carbonate products (i.e.,  $\text{FeCO}_3$  and  $\text{CaCO}_3$ ) occurred. This observation is in agreement with the study by El-Bellihi [53], where it has been stated that the decomposition of iron carbonate resulted in a peak at 495 °C. Stopic et al. [48] also discussed the thermal decomposition of their sample and identified that a temperature interval of 470–595 °C was associated with magnesium/iron carbonate decomposition. Furthermore, Mendoza et al. [47] mentioned that at 367 °C, siderite ( $\text{FeCO}_3$ ) begins to decompose and release carbon dioxide. Based on the DTG curve of the carbonated sample, some small peaks right before the large peak can be observed and, thus, can be attributed to the initial stage of iron carbonate decomposition. After the peak of iron carbonate decomposition, which leaves residue of iron oxide, a peak followed at about 630–700 °C for the carbonated sample, which could be related to the presence of ferric oxide ( $\text{Fe}_2\text{O}_3$ ) [51]. Both of the reactions occurred in the temperature interval 340–700 °C, which explains the large peak that appeared as two peaks, while the raw sample has only a single peak in the same temperature interval. The two peaks might be associated with the thermal decomposition of carbonate product followed by ferric oxide decomposition (carbonate product residue). Following the most distinctive peak is a smaller peak (fourth peak) in the temperature range of 700–1000 °C, where the DTG peaks for both samples are almost similar. However, the weight reduction of raw Fe-rich material is 1.95%, while carbonated waste experienced 2.32% weight reduction, which corresponds to the decarbonation of calcium carbonate [54]. In contrast to carbonated waste material with an overall weight loss of 16.3%, the overall weight reduction of raw waste material is low (8.71%), which implies that a new product was formed after the raw waste material underwent the carbonation process. The high weight loss observed in the carbonated Fe-rich waste sample compared to the raw sample confirms that a carbonation reaction has occurred and that a carbonate product was formed.

The smaller particle sizes of waste can aid carbon dioxide gas exchange and the process of carbonation for the entire mass of the waste sample [72]. Most studies in related fields have found similar results: smaller particle size was most feasible in increasing the carbon uptake capacity. Yan et al. [29] achieved 83.5% efficiency using particle sizes of <30 µm of wollastonite (40 bar, 150 °C). Azdarpour et al. [30] successfully obtained 5.76% and 12.53% Fe and Ca conversion efficiency using <45 µm of red gypsum samples with constant carbon dioxide pressure of 20 bar and temperature of 200 °C. Furthermore, decreasing the particle size can also optimize the leaching of  $\text{Mg}^{2+}$  ions up to 99% due to the escalating reaction rate of the substrate surface area [73]. Rates of conversion to a carbonate product from 24% to 74% were achieved through the reduction of particle size from <2 mm to <38 µm in 30 min of reaction time (19 bar and 100 °C) [74]. Accordingly, the surface area can be increased by grinding or sieving, making the particle size smaller but with more available surface area for the reaction to occur; this is also known as mechanical activation [24]. Although the uptake capacity obtained through this experiment was quite low, the results were comparable to that of using a high-energy reactor (high pressure and high-temperature system). Even though the carbonation experiment was conducted at ambient pressure (1 bar) and low temperature (80 °C), an uptake capacity of 3.97% can still be achieved for Fe-rich mine waste. Hence, the carbonation reaction of this waste has shown that smaller particle sizes can greatly affect the reaction process.

### 3.2.3. Influence of Reaction Temperature on Uptake Capacity

The influence of the reaction temperature on uptake capacity was studied by applying different reaction temperatures of 80 °C, 150 °C and 200 °C. At the same time, other parameters remained constant throughout the experiment, including 1 bar reaction pressure, 63 µm particle size, and pH 8.5. Sodium chloride and sodium bicarbonate, with concentrations of 1 M and 0.64 M, respectively, were added into 10 g of the sample before the carbonation experiment was carried out.

The average uptake capacities of 5 sampling locations over different temperatures of 80–200 °C are presented in Figure 9. Based on the figure, Fe uptake capacity (%) decreases with increasing temperature; this occurs similarly for Ca uptake capacity. Ca uptake capacity is 2.4%, 2.0% and 2.3% and Fe uptake is 3.3%, 2.7% and 2.5% for temperatures of 80 °C, 150 °C and 200 °C, respectively. Although it may seem unusual, it is not impossible to obtain this trend of results as opposed to an increase of uptake capacity, which was expected to be increased with increasing reaction temperature. Ukwattage et al. [75] have obtained similar findings, showing that the carbonation rate decreases at temperatures over 60 °C due to the decrease in carbon dioxide solubility in the solution. This can be explained by the opposite reaction to the two major stages of carbonation (i.e., leaching of metal ions and dissolution of carbon dioxide in the slurry) caused by the elevated reaction temperature. According to Huijgen et al. [74], metal ion leaching from a matrix probably proceeds at a faster rate in high temperatures. On the other hand, elevated temperature can inhibit the carbonate precipitation process owing to carbon dioxide solubility being reduced; hence, there is less available carbon dioxide that can react with the metal ions [76]. Thus, maintaining a suitable temperature for enough metal ions and carbon dioxide to be available is crucial to obtaining optimum results.

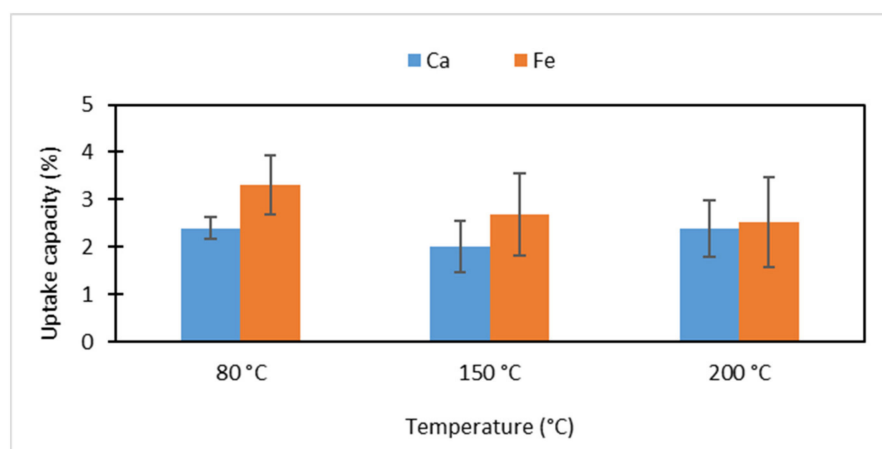


**Figure 9.** Average Ca and Fe uptake capacity (%) for different reaction temperatures of Fe-rich mine waste. Error bars represent standard error of the mean (SEM).

In theory, carbon uptake was expected to increase with temperature. A study by Chen et al. [77] supported the theory that temperature increment can aid metal ion extraction from the source, which eventually results in a positive effect on carbonate precipitation. Tai et al. [78] experienced an increase in the wollastonite carbonation rate from 30% to 75% over a reaction temperature of about 50 °C to 140 °C. With the assumption that wollastonite dissolution rate is the controlling factor, it was stated that the dissolution rate of the feedstock eventually increases with temperature. While this might be true, past studies have also proven that too high of a temperature can give undesirable results. Fagerlund et al. [79] stated that overly increased temperature can lower the final carbonation rate. Moreover, Azdarpour et al. [63] have reported that two distinct reactions were observed with an increase in temperature. It was found that while carbonate purity keeps increasing

with temperature, it started to decline at a temperature of 200 °C from 10.47% to 8.71% of iron carbonate at a 300 °C reaction temperature.

Based on Table 1, a reaction temperature of 80 °C has the highest Ca uptake capacity of 2.59% and 1.47% compared to a reaction temperature of 200 °C, which demonstrated an uptake capacity of 1.12% and 0.83% in tailings and waste dump, respectively. Ca uptake in a decreasing manner for pond 1 is achieved using a temperature of 200 °C, followed by 80 °C and 150 °C (i.e., 3.33%, 2.52% and 2.27%, respectively). For pond 2, the decreasing trend is at 150 °C followed by 200 °C and 80 °C (i.e., 3.99%, 3.91% and 2.68%, respectively), and for pond 3, the trend is 200 °C, 80 °C and 150 °C (i.e., 2.71%, 2.67% and 1.45, respectively). For Fe uptake capacity, pond 1 and waste dump have decreasing trends with increasing temperature. The Fe uptake capacity of pond 1 and waste dump are 2.77%, 1.07% and 0.89%, and 3.33%, 1.07% and 0.94% for reaction temperatures of 80 °C, 150 °C and 200 °C, respectively. Meanwhile, pond 1 and pond 2 have increasing capacities with increasing temperatures, demonstrating capacities of 5.66%, 5.71%, and 5.81%, and 2.85%, 3.45% and 3.50% for 80 °C, 150 °C and 200 °C, respectively. For tailings, the highest Fe uptake was achieved using a reaction temperature of 150 °C (2.05%), followed by 80 °C (1.95%) and 200 °C (1.45%), demonstrating a decreasing trend with temperature.

**Table 1.** Ca and Fe uptake capacity (%) of Fe-rich mine waste in different temperatures.

Sample	Temperature (°C)	Ca Uptake Capacity (%)	Fe Uptake Capacity (%)
Pond 1	80	2.52	2.77
	150	2.27	1.07
	200	3.33	0.89
Pond 2	80	2.68	5.66
	150	3.99	5.71
	200	3.91	5.81
Pond 3	80	2.67	2.85
	150	1.45	3.49
	200	2.71	3.50
Tailings	80	2.59	1.95
	150	1.04	2.05
	200	1.12	1.45
	80	1.46	3.33
Waste Dump	150	1.20	1.07
	200	0.83	0.94

Both Ca and Fe efficiency have shown some contradicting results in different sampling locations. Although the uptake capacity of pond 2 and pond 3 seems to increase with temperature, there was no dramatic increase in uptake capacity despite the temperature being increased from 80 °C to 200 °C. There was only a small difference in uptake capacity in pond 2, where 80 °C yielded an uptake capacity of 5.66% and 150 °C and 200 °C yielded uptake capacities of 5.71% and 5.81%, respectively. The Fe uptake capacity of tailings also seemed to increase up until 150 °C and decrease when the temperature was increased further to 200 °C. This shows that high temperature might slightly increase the uptake capacity; however, too high of a temperature might slow down the carbonation rate, yielding undesirable results. This can be seen in the Fe uptake capacity of tailings, where there were only small differences in uptake capacity between reaction temperatures of 80 °C (1.95%) and 150 °C (2.05%). This uptake capacity further decreased to 1.45% at a temperature of 200 °C. This shows that a reaction temperature of 80 °C was capable of achieving an uptake capacity that was comparable to higher operating temperatures.

In a nutshell, the optimum temperature for the carbonation reaction is different for each material depending on the feedstock characteristic and the operating conditions of the experiment. For this study, a reaction temperature of 80 °C can be considered a feasible temperature due to its comparable performance with higher operating temperatures

and the fact that it is non-energy extensive, which makes the carbonation process seem more attractive.

### 3.3. CO<sub>2</sub> Sequestration Capacity in Fe-Rich Waste Materials (g CO<sub>2</sub>/kg Fe-Rich Waste Material)

The carbon dioxide sequestration capacity in g of CO<sub>2</sub> per kg of waste material was calculated from weight loss in TGA. Figure 10a shows the sequestration capacity for Fe-rich mine waste, which was 83.8 g CO<sub>2</sub>/kg, 74.7 g CO<sub>2</sub>/kg and 55.8 g CO<sub>2</sub>/kg using particle sizes of 38 μm, 63 μm and 75 μm, respectively. The trend of increasing capacity with decreasing particle size provides a good indication for optimizing the carbonation reaction.

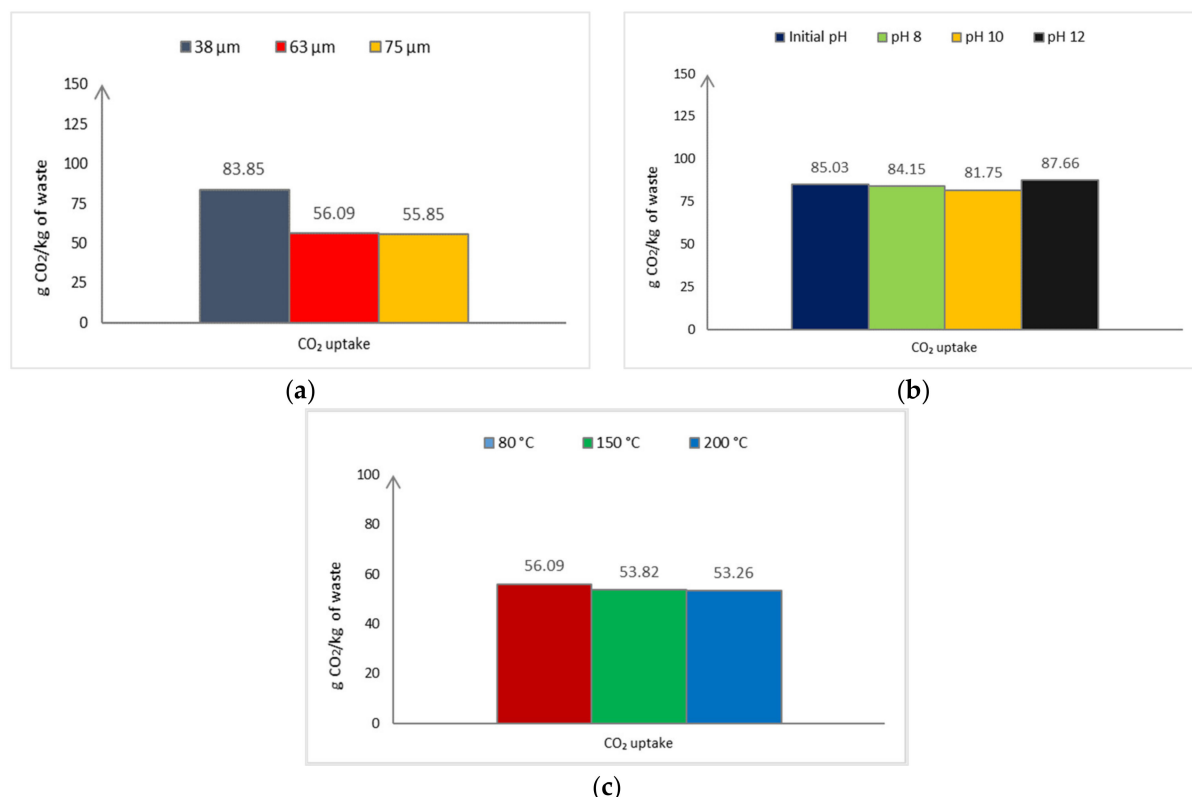


**Figure 10.** Carbon capture capacity (g/kg of waste) of Fe–rich mine waste in different (a) particle size, (b) pH condition and (c) reaction temperature.

Meanwhile, Figure 10b shows the sequestration capacity per kg of Fe-rich mine waste in different pH conditions. pH 12 seems to have the highest sequestration capacity of 87.6 g CO<sub>2</sub>/kg Fe-rich waste. This is similar to the uptake capacity (%), where pH 12 recorded the highest uptake. On the other hand, pH 10 does not seem favorable for the formation of FeCO<sub>3</sub>, which can be seen by the lowest sequestration capacity (81.7 g CO<sub>2</sub>/kg Fe-rich waste) in pH 10 conditions. This suggests that pH 10 might not be good for the reaction between CO<sub>2</sub> and FeO/Fe<sub>3</sub>O<sub>4</sub>.

In terms of temperature, Figure 10c shows that the carbon sequestration capacity of Fe-rich waste decreases when the reaction temperature increases. The sequestration capacities for reaction temperatures of 80 °C, 150 °C and 200 °C are 56.1 g CO<sub>2</sub>/kg, 53.8 g CO<sub>2</sub>/kg and 53.3 g CO<sub>2</sub>/kg, respectively. Several studies that focused on utilizing lower temperatures have experienced a similar trend. Ukwattage et al. [31] have stated that sequestration capacity was slightly reduced from 60 °C to 80 °C, and the optimum temperature for carbon sequestration was 50 °C for 29.5 g CO<sub>2</sub>/kg in 48 h. Decreasing carbonation with increasing temperature can be explained by the disruption of the precipitation process, such that the increase in temperature has caused the solubility of carbon dioxide gas into the solution, depleting the solubility of bicarbonate ion [74]. Although higher temperatures can

increase the leaching of Ca/Mg/Fe ions, the presence of bicarbonate ions is still needed for carbonate to precipitate. At a lower temperature of 80 °C, there was plenty of bicarbonate ions available in the solution from NaHCO<sub>3</sub> and the dissolution of carbon dioxide gas. However, when the temperature started to increase, the decrease in available bicarbonate ions caused the uptake capacity to decrease. Despite the fact that higher temperatures were expected to increase sequestration capacity, the present study has shown the opposite results. In this case, the waste material properties and the operating condition play an important role, as the carbonation process is highly dependent on feedstock characteristics.

In order to support whether the different parameters applied affect the uptake capacity (%), Kruskal–Wallis H tests at a 0.05% significance level were performed. The results for the Fe-rich mine waste sample shows that there was no statistically significant difference in uptake capacity using different pH conditions and reaction temperatures. This might suggest that the chosen pH range (i.e., pH 7–12) and temperatures (i.e., 80 °C, 150 °C, 200 °C) have more or less the same effect on the carbonation process because of its alkaline nature. Despite this, the slight change and trend observed cannot be ignored and might have explained the kinetic reaction involved in the process. However, a significant difference ( $p < 0.05$ ) in uptake capacity using different particle size fractions was found, where there was a statistically significant difference ( $p < 0.05$ ) between the mean ranks of at least one pair of groups. Dunn–Bonferroni pairwise tests revealed that there was a statistically significant difference in mean ranks between a particle size of 38 μm and a particle size of 75 μm. This means that using 38 μm or 75 μm particle size fractions will give different results regarding the uptake capacity.

Spearman's rank-order correlation test revealed that there was a statistically significant, negative correlation between uptake capacity (%) and particle size used ( $r = -0.487$ ,  $p = 0.006$ ), which suggests that using smaller particle size fractions will increase the uptake capacity of the Fe-rich mine waste sample.

### 3.4. Production of a Mineral Carbonation Product and Its Application

This section emphasizes the products of the mineral carbonation process (i.e., amount of CaCO<sub>3</sub> and FeCO<sub>3</sub> formed). Figure 11 shows the amount of carbonate product formed via the carbonation process. Throughout 1 h carbonation of Fe-rich mine waste, 0.44 g FeCO<sub>3</sub>/kg, 0.39 g FeCO<sub>3</sub>/kg and 0.29 g FeCO<sub>3</sub>/kg of waste were produced with particle sizes of 38 μm, 63 μm and 75 μm, respectively (Figure 11a). On the other hand, 0.43–0.46 g FeCO<sub>3</sub>/kg of Fe-rich mine waste was precipitated in pH conditions of 7–12 (Figure 11b), while 0.28–0.39 g FeCO<sub>3</sub>/kg was formed in reaction temperatures of 80–200 °C (Figure 11c).

The presence of carbonate minerals was confirmed by XRD analysis, as presented in Figure 12. In the carbonated sample, new peaks of magnetite (Fe<sub>3</sub>O<sub>4</sub>), siderite (FeCO<sub>3</sub>), iron carbonate hydroxide (Fe<sub>2</sub>(OH)<sub>2</sub>CO<sub>3</sub>), calcite (CaCO<sub>3</sub>) and aragonite (CaCO<sub>3</sub>) were found. Iron carbonate hydroxide is one of the only ferrous carbonate minerals besides siderite [80]. The minor peak of iron carbonate hydroxide, siderite, calcite and aragonite explains the low Ca and Fe uptake capacity obtained from the carbonation experiment, which also explains the presence of the same magnetite and hematite peak in the raw and carbonated samples. The reason for this is that only a small amount of magnetite was used during carbonation, resulting in low uptake capacity. The magnetite presence might be due to the thermal decomposition of hematite in the presence of CO<sub>2</sub> gases during carbonation reactions where the temperature was varied [52,64,65].

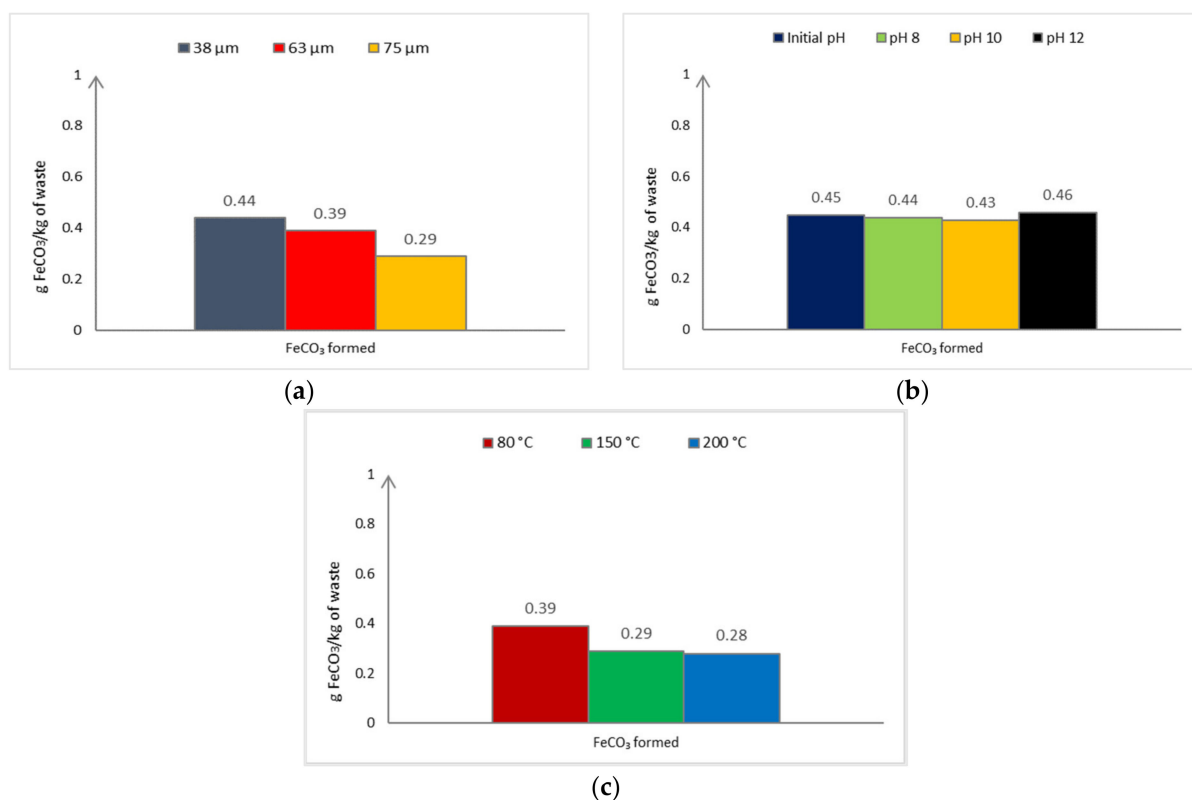


**Figure 11.** Carbonate product formed (g/kg of waste) of Fe-rich waste in different (a) particle size, (b) pH condition and (c) reaction temperature.

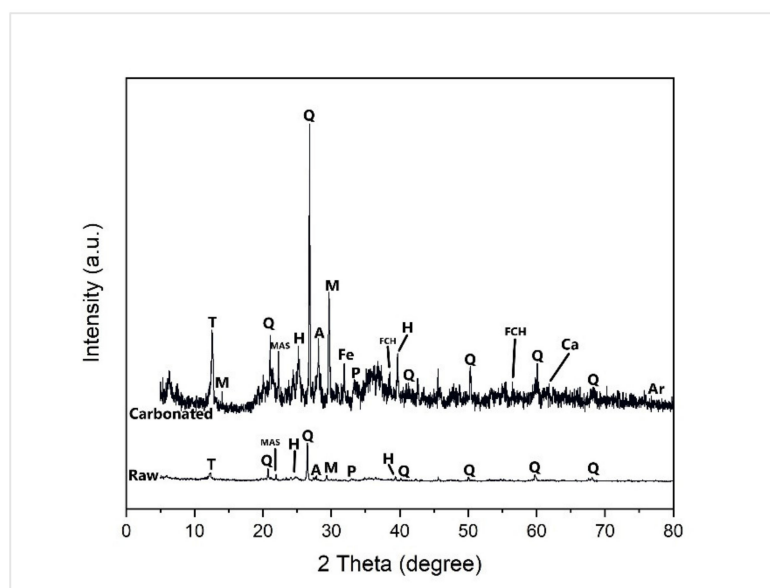


**Figure 12.** X-ray diffractogram patterns of raw and carbonated samples of Fe-rich mine waste. Labelled alphabet represents the minerals found in the waste: quartz (Q), anorthite (A), wollastonite (W), diopside (D), titanium Silicon (T), magnetite (M), perovskite (P), magnesium aluminium silicate (MAS), johannsenite (J), hematite (H), aragonite (Ar), siderite (Fe), iron carbonate hydroxide (FCH) and calcite (Ca).

The amount of carbonate product formed, which was further confirmed by XRD analysis, shows that carbonated products ( $\text{FeCO}_3$ ) were successfully sequestered from the mineral carbonation process, which indicates that mine waste can be a potential feedstock or agent

for carbon dioxide capture, i.e., transforming gaseous carbon dioxide into stable carbonates. The capability of the waste to produce carbonate products shows that it was able to act as a sequestration medium for a carbon capture application. For instance, this concept can be applied to the carbonation curing process in the production of cement-based materials (CBMs), such as in the brick-making process. The availability of silica, calcium and magnesium oxides in the mine waste makes it potential to use as a partial replacement for ordinary Portland cement (OPC), while at the same time acting as the sequestering agent.

One ton of manufactured OPC is approximately equivalent to one ton of carbon dioxide being released into the atmosphere [81]. To reduce the carbon footprint of OPC, an alternative low-carbon source that can act as an alternative supplementary cementitious material (SCM) and partially replace OPC is needed. Early assessment of the studied Fe-rich mine waste materials has shown that silica ( $\text{SiO}_2$ ) was present in high amounts. Eventually, if the waste is added as a partial cement replacement, this silica will react with the hydration product of the OPC, namely calcium hydroxide [ $\text{Ca}(\text{OH})_2$ ], forming calcium silicate hydrate (C-S-H); this is called a pozzolanic reaction [82]. In early stages, pozzolans act as a pore filler to make the material denser until  $\text{Ca}(\text{OH})_2$  is available, which is why it has been associated with slower strength development and highly improved overall strength [82]. Because this reaction is limited to the amount of  $\text{Ca}(\text{OH})_2$  from the OPC which is available to react with the  $\text{SiO}_2$  from the waste material [83], it is favorable for the reaction if the waste material contains calcium that can form  $\text{Ca}(\text{OH})_2$  so that it can further react with any unreacted  $\text{SiO}_2$ . Fe-rich mine waste contains calcium oxide, which makes it suitable to be used as an SCM.

Apart from having pozzolanic characteristics, the waste material also has the capability to produce carbonate products, which is important if carbonation curing is to be incorporated in the brick-making process. Carbonation curing is an advanced method of conventionally curing cement-based materials. Through carbonation curing, rapid hardening can occur when C-S-H is exposed to carbon dioxide, which can eventually improve the strength and properties of the materials [84].

Clearly, mineral carbonation using Fe-rich mine waste material can serve as a method for both capturing and storing carbon dioxide depending on the final destination of the carbonated product. In a brick making scenario with carbonation curing, for instance, carbon dioxide is captured and permanently stored in the brick while improving its strength. This approach specifically aims to reduce the carbon footprint associated with cement production while capturing existing carbon dioxide through the utilization of mine waste via carbonation curing. Through this process, carbon dioxide can be permanently captured and stored in the brick product. This is also in line with the concept of carbon-negative products (products which undergo a process where carbon is removed from the atmosphere). Therefore, partially replacing cement with mine waste material as an SCM can potentially reduce the use of natural resources and potentially be an agent for carbon dioxide sequestration.

### 3.5. Novelty and Contributions of Study

This study has proved the carbon capture potential of Fe-rich mine waste through mineral carbonation and by exploring the effects of different parameters to sequester more  $\text{CO}_2$ . While most of the previous research has focused on using Ca-Mg-rich minerals (e.g., serpentine, olivine, wollastonite), targeted host rock (granite, basalt), and industrial waste (cement, steel slag) as the raw materials for the mineral carbonation process, this study uses abandoned Fe-rich mine waste, which is an attempt to make use of mine waste material to capture  $\text{CO}_2$ . Furthermore, the utilization of iron oxide in the waste with its reaction with  $\text{CO}_2$  can give more insight to facilitate  $\text{CO}_2$  uptake, since most of the previous research emphasized the use of  $\text{MgO}$  and  $\text{CaO}$  for mineral carbonation because it is a more reactive mineral for the carbonation process and is also available in huge amounts. Furthermore, this study has also emphasized the importance of the mineralogical composition of such materials and explores the usefulness of the carbonated product

produced from the process, which can be integrated into cement-based material production that can act as a carbon sink to store CO<sub>2</sub> permanently. To that end, findings from this study will be beneficial in particular in terms of the mineralogical and chemical composition of waste material in association with its potential as feedstock for mineral carbonation. Moreover, the contribution towards environmental sustainability can be seen through the utilization of waste material as a resource for carbon sequestration that can help mitigate CO<sub>2</sub> emissions for the long term. In other words, this study promotes the sustainable use of resources that can be useful in producing green material, such as for construction purposes and for future mitigation strategies of mining-related issues (e.g., reducing waste production or contamination issues at mining sites).

#### 4. Conclusions

Based on initial characterization analysis, calcium oxide and iron oxide with percentage ranges of 7.19–15.24% and 39.6–62.9%, respectively, were expected to have a higher uptake capacity; however, low uptake capacity was obtained, i.e., 1.44–3.05% and 2.19–3.97% for Ca and Fe uptake capacity, respectively. This is probably due to the short time limitation for the carbonation reaction to proceed and the low amount of initial sample used (10 g) in the carbonation experiment. However, when compared to other studies, the uptake capacity and sequestration capacity obtained were found to be comparable to the capacities observed using high-energy reactors or using specific minerals as feedstock. Hence, it is recommended that the reaction time is prolonged and the amount of waste used increased so that the carbonation reaction process can take place without time and feedstock limitations.

From the carbonation experiment, it can be inferred that smaller particle size fractions (i.e., 38 µm), alkaline pH (i.e., pH 8–12) and a reaction temperature of 80 °C greatly benefit the carbonation reaction uptake capacity (3.97%) and sequestration capacity (83.80 g CO<sub>2</sub>/kg) under low pressure-temperature conditions (i.e., 1 bar and 80 °C). The presence of carbonate minerals was further confirmed by XRD analysis. Herein, this study has demonstrated the feasibility of reusing Fe-rich mine waste as feedstock for CCS/CCU via mineralization of carbon dioxide. This was mainly due to its alkaline nature and the fact that it contains Ca/Fe-bearing minerals that are reactive for carbon mineralization.

Therefore, this study has revealed that a substantial amount of carbon dioxide can be sequestered without using extensive energy during the reaction process. These findings would be useful in understanding more about the accelerated mineral carbonation process in order to develop a technology that is feasible for industrial-scale application, hence improving the emission reduction of carbon-extensive industries. The potential of reusing Fe-rich mine waste material on-site in high-emission industries could be further developed through extensive research where the end product could serve as a useful material in the construction sector. The waste materials which manifest pozzolanic properties, such as the one used in this study, are suitable as a partial replacement for cement in brick or concrete. On that account, these findings would be useful for research on utilizing the waste as a supplementary cementitious material to improve the properties of cement-based products in carbon storage applications. Therefore, this study has shown that Fe-rich mine waste materials can be reused for carbon sequestration, which is in line with the concept of green technology for environmental sustainability in climate mitigation strategies.

**Author Contributions:** Conceptualization, F.M.K. and A.M.A.; methodology, V.L.M.M. and N.A.A.R.; formal analysis, S.N.M.S.H. and V.L.M.M.; investigation, S.N.M.S.H. and V.L.M.M.; resources, S.N.M.S.H. and F.M.K.; data curation, V.L.M.M. and N.A.A.R.; writing—original draft preparation, V.L.M.M.; writing—review and editing, F.M.K.; visualization, N.A.A.R. and V.L.M.M.; supervision, F.M.K., A.M.A. and S.N.M.S.H.; project administration, F.M.K.; funding acquisition, F.M.K. All authors have read and agreed to the published version of the manuscript.

**Funding:** This research was funded by the Ministry of Higher Education Malaysia (MOHE), grant number KPM FRGS/1/2018/TK10/UPM/02/7 (FRGS 5540081) and Universiti Putra Malaysia, grant number IPS 9574900.

**Institutional Review Board Statement:** Not applicable.

**Informed Consent Statement:** Not applicable.

**Data Availability Statement:** Not applicable.

**Acknowledgments:** The authors would like to thank laboratory staff at the Centre for Research and Instrumentation (CRIM), Universiti Kebangsaan Malaysia, Bangi, Malaysia and Material Characterization Laboratory, Department of Chemical and Environmental Engineering, Universiti Putra Malaysia, Serdang, Malaysia for providing technical assistance for laboratory analysis.

**Conflicts of Interest:** The authors declare no conflict of interest.

## References

1. Oalkers, E.H.; Cole, D.R. Carbon Dioxide Sequestration: A Solution to a Global Problem. *Elements* **2008**, *4*, 305–310. [CrossRef]
2. Trends in Atmospheric Carbon Dioxide. National Oceanic and Atmospheric Administration (NOAA). Available online: [www.esrl.noaa.gov/gmd/ccgg/trends/](http://www.esrl.noaa.gov/gmd/ccgg/trends/) (accessed on 9 June 2018).
3. Trends in Atmospheric Carbon Dioxide. National Oceanic and Atmospheric Administration (NOAA). Available online: <https://gml.noaa.gov/ccgg/trends/mlo.html> (accessed on 10 January 2022).
4. Dumitru, O.A.; Austermann, J.; Polyak, V.J.; Fornós, J.J.; Asmerom, Y.; Ginés, J.; Ginés, A.; Onac, B.P. Constraints on global mean sea level during Pliocene warmth. *Nature* **2019**, *574*, 233–236. [CrossRef] [PubMed]
5. Brigham-Grette, J.; Melles, M.; Minyuk, P.; Andreev, A.; Tarasov, P.; DeConto, R.; Koenig, S.; Nowaczyk, N.; Wennrich, V.; Rosén, P.; et al. Pliocene warmth, polar amplification, and stepped pleistocene cooling recorded in NE Arctic Russia. *Science* **2013**, *340*, 1421–1427. [CrossRef]
6. Leung, D.Y.C.; Caramanna, G.; Maroto-Valer, M.M. An overview of current status of carbon dioxide capture and storage technologies. *Renew. Sustain. Energy Rev.* **2014**, *39*, 426–443. [CrossRef]
7. United State of Geological Survey (USGS). Carbon Sequestration to Mitigate Climate Change. 2008. Available online: <https://pubs.usgs.gov/fs/2008/3097/pdf/CarbonFS.pdf#page=1&zoom=auto,-99,798> (accessed on 24 June 2018).
8. IPCC. Carbon Dioxide Capture and Storage. In *IPCC Special Report Prepared by Working Group III of the Intergovernmental Panel on Climate Change*; Metz, B., Davidson, O., Coninck, H.D., Loos, M., Meyer, L., Eds.; Cambridge University Press: Cambridge, UK; New York, NY, USA, 2005; 442p.
9. Ashurst, P.R.; Hargitt, R.; Palmer, F. Chapter 3—Ingredients in Soft Drinks. In *Woodhead Publishing Series in Food Science, Technology and Nutrition, Soft Drink and Fruit Juice Problems Solved*, 2nd ed.; Philip, R.A., Hargitt, R., Palmer, F., Eds.; Woodhead Publishing: Sawston, UK, 2017; pp. 29–66. [CrossRef]
10. Alshalif, A.F.; Irwan, J.M.; Othman, N.; Al-Gheethi, A.A.; Shamsudin, S.; Nasser, I.M. Optimisation of carbon dioxide sequestration into bio-foamed concrete pores using *Bacillus tequilensis*. *J. CO<sub>2</sub> Util.* **2021**, *44*, 101412. [CrossRef]
11. Othman, F.E.C.; Yusof, N.; Samitsu, S.; Abdullah, N.; Hamid, M.F.; Nagai, K.; Abidin, M.N.Z.; Azali, M.A.; Ismail, A.F.; Jaafar, J.; et al. Activated carbon nanofibers incorporated metal oxides for CO<sub>2</sub> adsorption: Effects of different type of metal oxides. *J. CO<sub>2</sub> Util.* **2021**, *45*, 101434. [CrossRef]
12. Zhu, H.; Yu, K.; Li, V.C. Sprayable engineered cementitious composites (ECC) using calcined clay limestone cement (LC3) and PP fiber. *Cem. Concr. Compos.* **2021**, *115*, 103868. [CrossRef]
13. Kusin, F.M.; Hasan, S.N.M.S.; Hassim, M.A.; Molahid, V.L.M. Mineral carbonation of sedimentary mine waste for carbon sequestration and potential reutilization as cementitious material. *Environ. Sci. Pollut. Res.* **2020**, *27*, 12767–12780. [CrossRef]
14. Madhavi, K.B.; Venugopal, M.; Rajesh, V.; Suresh, K. Experimental Study on Bendable Concrete. *Int. J. Eng. Res. Tech.* **2016**, *5*, 501–504. [CrossRef]
15. Truong, C.C.; Mishra, D.K. Recent advances in the catalytic fixation of carbon dioxide to value-added chemicals over alkali metal salts. *J. CO<sub>2</sub> Util.* **2020**, *41*, 101252. [CrossRef]
16. Yi, Z.; Wang, T.; Guo, R. Sustainable building material from CO<sub>2</sub> mineralization slag: Aggregate for concretes and effect of CO<sub>2</sub> curing. *J. CO<sub>2</sub> Util.* **2020**, *40*, 101196. [CrossRef]
17. Kaliyavaradhan, S.K.; Ling, T.C.; Mo, K.H. CO<sub>2</sub> sequestration of fresh concrete slurry waste: Optimization of CO<sub>2</sub> uptake and feasible use as a potential cement binder. *J. CO<sub>2</sub> Util.* **2020**, *42*, 101330. [CrossRef]
18. Von der Assen, N.; Jung, J.; Bardow, A. Life-cycle assessment of carbon dioxide capture and utilization: Avoiding the pitfalls. *Energy Environ. Sci.* **2013**, *6*, 2721–2734. [CrossRef]
19. Centre for Low Carbon Future (CLCF). *Carbon Capture and Utilisation in the Green Economy: Using CO<sub>2</sub> to Manufacture Fuel, Chemicals and Materials*; Report Prepared by the Energy Research Centre of the Netherlands (ECN) and the University of Sheffield; Styring, P., Jansen, D., de Coninck, H., Reith, H., Armstrong, K., Eds.; Centre for Low Carbon Future: Yorkshire, UK, 2011; 60p.

20. Markewitz, P.; Kuckshinrichs, W.; Leitner, W.; Linssen, J.; Zapp, P.; Bongartz, R.; Schreiber, A.; Muller, T.E. Worldwide innovations in the development of carbon capture technologies and the utilization of CO<sub>2</sub>. *Energy Env. Sci.* **2012**, *5*, 7281–7305. [CrossRef]
21. Yu, K.M.K.; Curcic, I.; Gabriel, J.; Tsang, S.C.E. Recent advances in CO<sub>2</sub> capture and utilization. *ChemSusChem* **2008**, *1*, 893–899. [CrossRef] [PubMed]
22. Steynberg, A.P. Introduction to Fischer-Tropsch Technology. In *Studies in Surface Science and Catalysis*; Steynberg, A.P., Dry, M., Eds.; Elsevier B.V.: Amsterdam, The Netherland, 2004; Volume 152, pp. 1–63. [CrossRef]
23. Lackner, K.S.; Wendt, C.H.; Butt, D.P.; Joyce, E.L.; Sharp, D.H. Carbon dioxide disposal in carbonate minerals. *Energy* **1995**, *20*, 1153–1170. [CrossRef]
24. Jacobs, A.D.; Hitch, M. Experimental mineral carbonation: Approaches to accelerate CO<sub>2</sub> sequestration in mine waste materials. *Int. J. Min. Reclam. Environ.* **2011**, *25*, 321–331. [CrossRef]
25. Bobicki, E.R.; Liu, Q.; Xu, Z.; Zeng, H. Carbon capture and storage using alkaline industrial wastes. *Prog. Energy Combust. Sci.* **2012**, *38*, 302–320. [CrossRef]
26. Sanna, A.; Uibb, M.; Caramanna, G.; Kuusik, R.; Maroto-Valer, M.M. A Review of Mineral Carbonation Technologies to Sequester CO<sub>2</sub>. *Chem. Soc. Rev.* **2014**, *43*, 8049–8080. [CrossRef]
27. Gerdemann, S.J.; Dahlin, D.C.; O'Connor, W.K.; Penner, L.R.; Rush, G.E. Ex-situ and in-situ mineral carbonation as a means to sequester carbon dioxide. In Proceedings of the 21st Annual International Pittsburgh Coal Conference, Osaka, Japan, 13–17 September 2004; Pittsburgh Coal Conference (PCC): Pittsburgh, PA, USA, 2004.
28. Teir, S.; Eloneva, S.; Fogelholm, C.J.; Zevenhoven, R. Stability of calcium carbonate and magnesium carbonate in rainwater and nitric acid solutions. *Energy Convers. Manag.* **2006**, *47*, 3059–3068. [CrossRef]
29. Yan, H.; Zhang, J.; Zhao, Y.; Liu, R.; Zheng, C. CO<sub>2</sub> sequestration by direct aqueous mineral carbonation under low-medium pressure conditions. *J. Chem. Eng. Jpn.* **2015**, *48*, 937–946. [CrossRef]
30. Azdarpour, A.; Karaei, M.A.; Hamidi, H.; Mohammadian, E.; Honarvar, B. CO<sub>2</sub> sequestration through direct aqueous mineral carbonation of red gypsum. *Petroleum* **2018**, *4*, 398–407. [CrossRef]
31. Ukwattage, N.L.; Ranjith, P.G.; Li, X. Steel-making slag for mineral sequestration of carbon dioxide by accelerated carbonation. *Meas. J. Int. Meas. Confed.* **2017**, *97*, 15–22. [CrossRef]
32. Carbon Cure Technologies Inc. CarbonCure’s Sustainable Concrete Solution—Concrete Technology Reducing Carbon Impact. *Carbon Cure Technologies*. Available online: <https://www.carboncure.com/> (accessed on 8 May 2020).
33. Pan-United Corporation Ltd. Sustainability through Low-Carbon Concrete Solutions. Available online: <https://www.panunited.com.sg/page/sustainability/> (accessed on 12 May 2020).
34. Mineral Carbonation International. Decarbonizing Global Industry. Available online: <https://www.mineralcarbonation.com/> (accessed on 8 May 2020).
35. Carbon8 Systems Ltd. Carbon8 Systems. Available online: <http://c8s.co.uk/> (accessed on 8 May 2020).
36. Solidia Technologies Inc. Solidia Technologies. Available online: <https://solidiatech.com/> (accessed on 8 May 2020).
37. Vallero, D.A.; Blight, G. Mine Waste: A brief overview of origins, quantities, and methods of storage. In *Waste Streams (and Their Treatment)*, 2nd ed.; Elsevier Inc.: San Diego, CA, USA, 2019; pp. 129–151. [CrossRef]
38. Hitch, M.; Ballantyne, S.M.; Hindle, S.R. Revaluing mine waste rock for carbon capture and storage. *Int. J. Mining Reclam. Env.* **2010**, *24*, 64–79. [CrossRef]
39. Mohd-Isha, N.S.; Kusin, F.M.; Kamal, N.M.A.; Hasan, S.N.M.S.; Molahid, V.L.M. Geochemical and mineralogical assessment of sedimentary limestone mine waste and potential for mineral carbonation. *Environ. Geochem. Health* **2021**, *43*, 2065–2080. [CrossRef]
40. Molahid, V.L.M.; Kusin, F.M.; Kamal, M.N.A.; Hasan, S.N.M.S.; Ramli, N.A.A.; Abdullah, A.M.; Ashaari, Z.H.A. Carbon sequestration of limestone mine waste through mineral carbonation and utilization as supplementary cementitious material. *Int. J. Integr. Eng.* **2021**, *13*, 311–320.
41. Hasan, S.N.M.S.; Kusin, F.M. Potential of mining waste from metallic mineral industry for carbon sequestration. *IOP Conf. Ser. Mater. Sci. Eng.* **2018**, *458*, 012013. [CrossRef]
42. Hasan, S.N.M.; Kusin, F.; Jusop, S.; Yusuff, F. Potential of Soil, Sludge and Sediment for Mineral Carbonation Process in Selinsing Gold Mine, Malaysia. *Minerals* **2018**, *8*, 257. [CrossRef]
43. Ramli, N.A.A.; Kusin, F.M.; Molahid, V.L.M. Influencing factors of the mineral carbonation process of the iron ore mining waste in sequestering atmospheric carbon dioxide. *Sustainability* **2021**, *13*, 1866. [CrossRef]
44. Smith, K.S.; Hageman, P.L.; Ramsey, C.A.; Wildeman, T.R.; Ranville, J.F. Reconnaissance sampling and characterization of mine-waste material. In Proceedings of the US Environmental Protection Agency Hard Rock Mining 2006 Conference, Tucson, AZ, USA, 14–16 November 2006; pp. 14–16.
45. BS 1377-3; Method of Test for Soils for Civil Engineering Purposes—Part 3: Chemical and Electro-Chemical Test. British Standards: London, UK, 1990.
46. Eikeland, E.; Blichfeld, A.B.; Tyrsted, C.; Jensen, A.; Iversen, B.B. Optimized carbonation of magnesium silicate mineral for CO<sub>2</sub> storage. *ACS Appl. Mater. Interfaces* **2015**, *7*, 5258–5264. [CrossRef]
47. Mendoza, E.Y.M.; Santos, A.S.; López, E.V.; Drozd, V.; Durygin, A.; Chen, J.; Saxena, S.K. Siderite formation by mechanochemical and high pressure-high temperature processes for CO<sub>2</sub> capture using iron ore as the initial sorbent. *Processes* **2019**, *7*, 735. [CrossRef]

48. Stopic, S.; Dertmann, C.; Modolo, G.; Kegler, P.; Neumeier, S.; Kremer, D.; Wotruba, H.; Etzold, S.; Telle, R.; Rosani, D.; et al. Synthesis of magnesium carbonate via carbonation under high pressure in an autoclave. *Metals* **2018**, *8*, 993. [[CrossRef](#)]
49. Revathy, T.D.R.; Palanivelu, K.; Ramachandran, A. Direct mineral carbonation of steelmaking slag for CO<sub>2</sub> sequestration at room temperature. *Environ. Sci. Pollut. Res.* **2016**, *23*, 7349–7359. [[CrossRef](#)] [[PubMed](#)]
50. El-hassan, H.; Shao, Y. Early carbonation curing of concrete masonry units with Portland limestone cement. *Cem. Concr. Compos.* **2015**, *62*, 168–177. [[CrossRef](#)]
51. Kawigraha, A.; Soedarsono, J.W.; Harjanto, S.; Pramusanto. Thermogravimetric analysis of the reduction of iron ore with hydroxyl content. *Adv. Mater. Res.* **2013**, *774–776*, 682–686. [[CrossRef](#)]
52. Qu, Y.; Yang, Y.; Zou, Z.; Zeilstra, C.; Meijer, K.; Boom, R. Thermal decomposition behaviour of fine iron ore particles. *ISIJ Int.* **2014**, *54*, 2196–2205. [[CrossRef](#)]
53. El-Bellahi, A.A. Kinetics of thermal decomposition of iron carbonate. *Egypt. J. Chem.* **2010**, *53*, 871–884. [[CrossRef](#)]
54. Ramachandran, V.S. Thermal Analysis. In *Handbook of Analytical Techniques in Concrete Science and Technology*, 2nd ed.; Ramachandran, V.S., Beaudoin, J.J., Eds.; William Andrew Publishing: Norwich, NY, USA, 2001; pp. 127–173. [[CrossRef](#)]
55. Alvarez, J.; Navarro, I.; García Casado, P. Thermal, mineralogical and chemical studies of the mortars used in the cathedral of Pamplona (Spain). *Thermochim. Acta* **2000**, *365*, 177–187. [[CrossRef](#)]
56. Moropoulou, A.; Bakolas, A.; Bisbikou, K. Characterization of ancient, byzantine and later historic mortars by thermal and X-ray diffraction techniques. *Thermochim. Acta* **1995**, *269–270*, 779–795. [[CrossRef](#)]
57. Hemmati, A.; Shayegan, J.; Bu, J.; Yeo, T.Y.; Sharratt, P. Process optimization for mineral carbonation in aqueous phase. *Int. J. Mineral. Processing* **2014**, *130*, 20–27. [[CrossRef](#)]
58. Prigobbe, V.; Hänenchen, M.; Werner, M.; Baciocchi, R.; Mazzotti, M. Mineral carbonation process for CO<sub>2</sub> sequestration. *Energy Procedia* **2009**, *1*, 4885–4890. [[CrossRef](#)]
59. Park, A.H.A.; Fan, L.S. CO<sub>2</sub> mineral sequestration: Physically activated dissolution of serpentine and pH swing process. *Chem. Eng. Sci.* **2004**, *59*, 5241–5247. [[CrossRef](#)]
60. Allahverdi, A.; Kani, E.N. Use of construction and demolition waste (CDW) for alkali-activated or geopolymers cements. In *Handbook of Recycled Concrete and Demolition Waste*; Pacheco-Torgal, F., Tam, V.W.Y., Labrincha, J.A., Ding, Y., de Brito, J., Eds.; Woodhead Publishing: Sawston, UK, 2013; pp. 439–475. [[CrossRef](#)]
61. Fantucci, H.; Sidhu, J.S.; Santos, R.M. Mineral Carbonation as an Educational Investigation of Green Chemical Engineering Design. *Sustainability* **2019**, *11*, 4156. [[CrossRef](#)]
62. Matson, M.L.; Orbaek, A.W. Chapter 18 Living in a Materials World. In *Solid State Chemistry in Inorganic Chemistry for Dummies*; John Wiley & Sons, Inc.: Hoboken, NJ, USA, 2013; pp. 287–304.
63. Azdarpour, A.; Asadullah, M.; Junin, R.; Manan, M.; Hamidi, H.; Mohammadian, E. Direct carbonation of red gypsum to produce solid carbonates. *Fuel Process. Tech.* **2014**, *126*, 429–434. [[CrossRef](#)]
64. Yu, J.; Han, Y.; Li, Y.; Gao, P.; Li, W. Mechanism and Kinetics of the Reduction of Hematite to Magnetite with CO-CO<sub>2</sub> in a Micro-Fluidized Bed. *Minerals* **2017**, *7*, 209. [[CrossRef](#)]
65. Yu, J.; Han, Y.; Li, Y.; Gao, P. Growth behavior of the magnetite phase in the reduction of hematite via a fluidized bed. *Int. J. Miner. Metall. Mater.* **2019**, *26*, 1231–1238. [[CrossRef](#)]
66. Walker, R.D. Iron Processing. Encyclopedia Britannica. 2017. Available online: <https://www.britannica.com/technology/iron-processing> (accessed on 5 October 2020).
67. Olsson, J.; Stripp, S.L.S.; Gislason, S.R. Element scavenging by recently formed travertine deposits in the alkaline springs from the Oman Samail Ophiolite. *Miner. Mag.* **2014**, *78*, 1479–1490. [[CrossRef](#)]
68. Magbitang, R.A.; Lamorena, R.B. Carbonate formation on ophiolitic rocks at different pH, salinity and particle size conditions in CO<sub>2</sub>-sparged suspensions. *Int. J. Ind. Chem.* **2016**, *7*, 359–367. [[CrossRef](#)]
69. Eloneva, S.; Teir, S.; Revitzer, H.; Salminen, J.; Said, A.; Fogelholm, C.; Zevenhoven, R. Reduction of CO<sub>2</sub> Emissions from Steel Plants by Using Steelmaking Slags for Production of Marketable Calcium Carbonate. *Process. Metall.* **2009**, *80*, 415–421. [[CrossRef](#)]
70. Wang, W.; Hu, M.; Zheng, Y.; Wang, P.; Ma, C. CO<sub>2</sub> Fixation in Ca<sup>2+</sup>-/Mg<sup>2+</sup>-Rich Aqueous Solutions through Enhanced Carbonate Precipitation. *Ind. Eng. Chem. Res.* **2011**, *50*, 8333–8339. [[CrossRef](#)]
71. Cruz-Navarro, D.S.; Mugica-Álvarez, V.; Gutiérrez-Arzaluz, M.; Torres-Rodríguez, M. CO<sub>2</sub> capture by alkaline carbonation as an alternative to a circular economy. *Appl. Sci.* **2020**, *10*, 863. [[CrossRef](#)]
72. Suescum-Morales, D.; Kalinowska-Wichrowska, K.; Fernández, J.M.; Jiménez, J.R. Accelerated carbonation of fresh cement-based products containing recycled masonry aggregates for CO<sub>2</sub> sequestration. *J. CO<sub>2</sub> Util.* **2021**, *46*, 101461. [[CrossRef](#)]
73. Rahmani, O.; Highfield, J.; Junin, R.; Tyrer, M.; Azdarpour, A.B. Experimental investigation and simplistic geochemical modeling of co<sub>2</sub> mineral carbonation using the mount tawai peridotite. *Molecules* **2016**, *21*, 353. [[CrossRef](#)] [[PubMed](#)]
74. Huijgen, W.J.J.; Comans, R.N.J. *Carbon Dioxide Sequestration by Mineral Carbonation: Literature Review Update 2003–2004*, ECN-C-05-022; Energy Research Centre of The Netherlands: Petten, The Netherlands, 2005.
75. Ukwattage, N.L.; Ranjith, P.G.; Yellishetty, M.; Bui, H.H.; Xu, T. A laboratory-scale study of the aqueous mineral carbonation of coal fly ash for CO<sub>2</sub> sequestration. *J. Clean. Prod.* **2014**, *103*, 665–674. [[CrossRef](#)]
76. Gerdemann, S.J.; O'Connor, W.K.; Dahlin, D.C.; Penner, L.R.; Rush, H. Ex situ aqueous mineral carbonation. *Env. Sci. Tech.* **2007**, *41*, 2587–2593. [[CrossRef](#)]

77. Chen, Z.Y.; O'Connor, W.K.; Gerdemann, S.J. Chemistry of aqueous mineral carbonation for carbon sequestration and explanation of experimental results. *Environ. Prog.* **2006**, *25*, 161–166. [[CrossRef](#)]
78. Tai, C.Y.; Chen, W.R.; Shih, S.M. Factors affecting wollastonite carbonation under CO<sub>2</sub> supercritical conditions. *Am. Inst. Chem. Eng.* **2005**, *52*, 292–299. [[CrossRef](#)]
79. Fagerlund, J.; Nduagu, E.; Romão, I.; Zevenhoven, R. CO<sub>2</sub> fixation using magnesium silicate minerals part 1: Process description and performance. *Energy* **2012**, *41*, 184–191. [[CrossRef](#)]
80. Koo, T.; Kim, J. Controls on the Formation and Stability of Siderite (FeCO<sub>3</sub>) and Chukanovite (Fe<sub>2</sub>(CO<sub>3</sub>)(OH)<sub>2</sub>) in Reducing Environment. *Minerals* **2020**, *10*, 156. [[CrossRef](#)]
81. Wang, D.L.; Chen, M.L.; Tsang, D.D.C.W. Green remediation by using low-carbon cement-based stabilization/solidification approaches. In *Sustainable Remediation of Contaminated Soil and Groundwater*; Elsevier Inc.: San Diego, CA, USA, 2020; pp. 93–118. [[CrossRef](#)]
82. Kamau, J.; Ahmed, A. Performance of Ternary Corncob Ash and Anthill Soil Concrete in Sulfate Solutions. *Eur. J. Eng. Res. Sci.* **2017**, *2*, 12. [[CrossRef](#)]
83. Ahmed, A.; Kamau, J.; Pone, J.; Hyndman, F.; Fitriani, H. Chemical Reactions in Pozzolanic Concrete. *Mod. Approaches Mater. Sci.* **2019**, *1*, 128–133. [[CrossRef](#)]
84. Zhang, D.; Ghouleh, Z.; Shao, Y. Review on carbonation curing of cement-based materials. *J. CO<sub>2</sub> Util.* **2017**, *21*, 119–131. [[CrossRef](#)]